



Klein, J., Ramirez-Torres, A., Ericsson, A., Huang, Y., Breuil, B., Siwy, J., Mischak, H., Peng, X.-R., Bascands, J.-L., and Schanstra, J. P. (2016) Urinary peptidomics provides a noninvasive humanized readout of diabetic nephropathy in mice. *Kidney International*, 90(5), pp. 1045-1055. (doi: [10.1016/j.kint.2016.06.023](https://doi.org/10.1016/j.kint.2016.06.023))

This is the author's final accepted version.

There may be differences between this version and the published version. You are advised to consult the publisher's version if you wish to cite from it.

<http://eprints.gla.ac.uk/132217/>

Deposited on: 2 February 2017

## **Non-invasive humanized readout of diabetic nephropathy in mice using urinary peptidomics**

Julie Klein<sup>1,2,†</sup>, Adela Ramirez-Torres<sup>3,†</sup>, Anette Ericsson<sup>4</sup>, Yufeng Huang<sup>5</sup>, Benjamin Breuil<sup>1,2</sup>, Justyna Siwy<sup>3</sup>, Harald Mischak<sup>3,6</sup>, Xiao-Rong Peng<sup>4</sup>, Jean-Loup Bascands<sup>1,2,\*</sup> and Joost P Schanstra<sup>1,2,\*</sup>

<sup>1</sup> Institut National de la Santé et de la Recherche Médicale (INSERM), U1048, Institute of Cardiovascular and Metabolic Disease, Toulouse, France.

<sup>2</sup> Université Toulouse III Paul-Sabatier, Toulouse, France.

<sup>3</sup> Mosaiques diagnostics & therapeutics, Hannover, Germany.

<sup>4</sup> Cardiovascular & Metabolic Disease Innovative Medicines, AstraZeneca R&D, Mölndal, Sweden.

<sup>5</sup> Department of Medicine, Division of Nephrology, University of Utah School of Medicine, Salt Lake City, USA.

<sup>6</sup> BHF Glasgow Cardiovascular Research Centre, Institute of Cardiovascular and Medical Sciences, Faculty of Medical, Veterinary and Life Sciences, University of Glasgow, Glasgow, UK.

†Equal contribution.

**Running head:** Humanized readout of nephropathy

\*Corresponding authors: [joost-peter.schanstra@inserm.fr](mailto:joost-peter.schanstra@inserm.fr) and [jean-loup.bascands@inserm.fr](mailto:jean-loup.bascands@inserm.fr)

INSERM U1048, Institute of Metabolic and Cardiovascular Diseases

1 avenue Jean Poulhes

BP84225 31432 Toulouse Cedex 4

France

## **ABSTRACT**

Diabetic nephropathy (DN) is among the most frequent complications of diabetes and the first cause of end-stage renal disease. Despite being successful in animal models, the majority of clinical trials for novel drugs targeting DN failed. This lack of translational value may in part be due to an inadequate comparability of human disease and animal models that often capture only a few aspects of disease. Here we overcome this limitation by developing a multi-molecular non-invasive humanized readout of DN based on urinary peptidomics. The disease-modified urinary peptides of two type 2 diabetic (T2D) DN mouse models were identified and compared with previously validated urinary peptide markers of DN in humans to generate a classifier composed of 21 ortholog peptides. This classifier predicted the response to disease and treatment with inhibitors of the renin-angiotensin system (RASi) in mice. The humanized classifier was significantly correlated with glomerular lesions. Using a human T2D validation cohort consisting of 207 patients, the classifier also distinguished between patients with and without DN, and response to RASi. Our approach demonstrates that a combination of multiple molecular features similar in both human and animal disease could provide a step change in translational drug discovery research in T2D-DN nephropathy.

**Keywords:** diabetic nephropathy, urine, proteomic analysis, albuminuria, ACEi.

## INTRODUCTION

Diabetic nephropathy (DN) is among the most frequent complications of diabetes <sup>1</sup> and recent evidence shows that kidney involvement is the main determinant of the increased risk of death in diabetic patients <sup>2</sup>. Despite significant advances in the understanding of the molecular mechanisms of type 2 diabetic (T2D, accounting for 90-95% of the diabetes cases) DN, the current standard-of-care is, however, still based on achieving blood pressure control by use of inhibitors of the renin-angiotensin system (RASi) on top of glycemic control. While slowing down the progression of DN in most cases, this treatment does not halt the ineluctable progression to end stage renal disease (ESRD, <sup>3</sup>). Therefore new drugs specifically targeting the DN pathophysiology are needed to reduce the burden of this disease. The translation of the extensive knowledge and plethora of potential targets <sup>4</sup> obtained in animal models of DN and other diseases to the clinic has been extremely limited <sup>3, 4</sup>. This has been attributed to the fact that: i) human pathophysiology and drug susceptibility are often not adequately captured by animal models <sup>5, 6</sup>, ii) readouts used in preclinical studies are usually different from the required endpoints in clinical trials <sup>7</sup>, or, iii) those readouts are based on a single molecule or phenotypic trait, not sufficient to assess pathology in detail and identify clinically valuable potential drug target (Fig. 1A) <sup>8, 9</sup>. Ways have been developed to circumvent these concerns mainly in the field of cancer and immunology by the development of humanized mouse models <sup>10</sup>. An alternative to the development of these humanized animal models, which is technically complicated and not always feasible in the context of many complex diseases such as DN, might be the optimization of the experimental readout based on a panel of molecular features that are

identical in both human and animal disease ignoring the non-human animal disease related traits (Fig. 1B).

While a multitude of animal models of DN exist<sup>11</sup>, the most frequently used models of T2D DN are the BTBRob/ob mice<sup>12</sup> and uninephrectomized db/db mice on a C57BLKS background (UNxdb/db,<sup>11</sup>). These two models are obese insulin resistant DN models due to leptin or leptin receptor deficiency respectively, displaying renal features similar to that observed in humans, including progressive albuminuria with advanced glomerular lesions and mild focal interstitial fibrosis. In addition, standard-of-care treatment using RASi confers renoprotection in these models<sup>13, 14</sup>. However this resemblance to human DN relies on albuminuria and histology, and often lacks any established molecular similarity; moreover, access to histological data requires animal sacrifice, which is costly, time consuming, and does not allow for longitudinal follow-up. In humans, current non-invasive readouts of progression of DN are based on the urinary albumin excretion rate (AER) and/or estimation of the glomerular filtration rate (eGFR) using serum creatinine. However, reduction of AER is not always correlated with complete reversal of all phenotypic and *in situ* changes observed in preclinical mouse models of DN<sup>13</sup>. Moreover, while routinely performed in humans, eGFR assessment in mice is of little comparative value, because in mice 35-50% of the creatinine is secreted and not attributable to the glomerular filtration<sup>15</sup>. Although methods for GFR measurement, based on fluorescent inulin clearance, have been developed for mice, these are still invasive (and cannot be repeated frequently,<sup>16</sup>) and will not detect small changes in renal function.

We and others have shown that urine is a rich and non-invasive source of biomarkers of disease in humans<sup>17-19</sup>. Mass spectrometry-based analysis of the endogenous urinary peptidome (i.e.,

not generated by trypsin digestion) allows the assessment of thousands of urinary peptides at once. Combined in multi-molecular classifiers of tens to hundreds of peptides, these urinary peptides have proven their ability to faithfully describe complex diseases including kidney disease<sup>17, 20</sup>, cardiovascular disease<sup>21</sup>, graft-versus-host disease<sup>22</sup>, and cholangiocarcinoma<sup>23</sup>. A successful example of the use of urinary peptides was the development of a urinary peptide based classifier for chronic kidney disease (CKD). Capillary electrophoresis coupled to mass spectrometry (CE-MS) was used to study the urinary peptidome of 230 patients compared to 379 healthy control subjects and led to the identification of a panel of 273 peptides associated with advanced CKD<sup>24</sup>. These 273 peptides combined into a classifier, termed CKD273, was subsequently validated for its capacity to detect CKD in independent cross-sectional studies with over 2000 patients including a significant number of patients (~70%) with diabetes<sup>25-28</sup>. Although initially designed for the detection of CKD, employment of the classifier also allowed prediction of progression of CKD in patients with CKD derived from different aetiologies<sup>28, 29</sup>, including patients with DN<sup>30, 31</sup>.

Based on this knowledge and the available urinary peptide classifiers in human for DN, the aim of the current study was to develop the first humanized multimarker readout in animal models of DN, using urinary peptidome analysis to improve on the translatability of the results obtained in animal models to the clinic for this disease. We showed that this multimarker model predicted the response to disease and standard-of-care treatment of DN in mice and in diabetic patients and outperformed the standard readout of DN in the mouse models.

## RESULTS

**The biological parameters, histology and urinary peptidome are highly comparable in response to DN and standard-of-care treatment in BTBRob/ob and UNxdb/db mice.**

With the aim to avoid strain- or mutation specific urinary peptide markers and to determine whether a generic DN peptidome readout in mice exists, we first analyzed the similarity of BTBRob/ob and the UNxdb/db mouse. BTBRob/ob and UNxdb/db mice demonstrated hyperglycemia with elevated blood glucose and glycated haemoglobin levels (Table 1) and increased body weights (not shown). This was accompanied by renal lesions as shown by the increased urinary albumin excretion rate (AER) (Fig. 2A) and glomerular PAS-positive material, indicative of glomerulosclerosis (Fig. 2B and C). In both models enalapril, a standard-of-care drug inhibiting the renin-angiotensin system (RASi), significantly reduced AER and glomerular lesions (Fig. 2A-C), without altering blood glucose or glycosylated haemoglobin levels (Table 1). The urinary peptidome of these two mouse strains was analyzed using CE-MS leading to the identification of 129 and 158 (Fig. 2D) sequenced peptides with significantly altered urinary excretion levels when employing multiple testing in the BTBRob/ob and the UNxdb/db DN mouse models compared to non diabetic control mice, respectively (Supplementary Table 1 and 2). Forty-eight identical peptides were modified with same regulation pattern in both models representing 30-37% of the observed peptides with different urinary abundance in DN (Fig. 2E). Most of the urinary peptides were collagen fragments (collagen type I alpha-1 and type III alpha-1 chains), similar to what has been found in humans with DN and CKD<sup>24, 32</sup>. Peptide fragments from other proteins, including complement factor D, uromodulin and pro-epidermal growth factor were also among the peptides of which the urinary abundance was modified in

DN (Supplementary Table 3). Using an approach that we have previously developed for the rat<sup>33</sup>, we identified 64 and 72 similar (orthologs) peptides in the human CKD273 classifier and in BTBRob/ob and UNxdb/db mice respectively, showing high molecular similarity between the mouse models and human DN. Treatment with RASi modified the urinary secretion of 11 peptides in BTBRob/ob mice, 18 peptides in the UNxdb/db DN mouse model (Supplementary Table 1 and 2). Four of the peptides modified by RASi were identical in both strains (Fig. 2F and Supplementary Table 4). Counterintuitive regulation of 2 of these 4 peptides was observed after RASi as RASi amplified the DN-induced changes for Napsin-A or SOX-6 fragments. Similar observations were reported in the past, where RASi was shown to exacerbate disease-induced changes while improving kidney function and histology<sup>34</sup>.

#### **Development of a humanized urinary peptide based classifier in T2D nephropathy mice.**

These data indicate that consistent changes were induced both by disease and treatment in these different strains. To obtain a generic (*eg* mutation independent) DN mouse urinary peptidome profile, we combined the data from the BTBRob/ob and UNxdb/db mice and their respective non-diabetic controls. Individual samples from non-diabetic and diabetic mice of the two strains were randomly assigned to a discovery or validation cohort (Table 2). The discovery cohort consisted of 10 non-diabetic, 10 DN, and 8 DN mice treated with RASi (Table 2). Ninety-two sequenced peptides displayed significantly altered urinary excretion levels between DN and non-diabetic and/or between treated and untreated DN mice (Supplementary Table 5), including 42 out of the 51 overlapping peptides previously identified in the two strains separately (Fig. 2E). These 92 peptides were confirmed to be mainly fragments of collagens. We



next identified the mouse peptides that could consistently reflect human disease by comparing the orthology of mouse urine peptide sequences to that of the 273 peptides in the CKD273-classifier (Fig. 1B, left panel). Among the 92 peptides significantly associated with DN in the mouse, 40 were orthologs (44%, Supplementary Table 5), again supporting high molecular similarity between human disease and these preclinical DN mouse models. Using support vector machines<sup>24</sup>, 21 mouse orthologs that had the best association to DN or RASi treatment were combined in a urine peptide classifier (Supplementary Table 6). This 21 peptide classifier included four peptides (Supplementary Table 6) which were uniquely changed after RASi and were not modified by DN. In this mouse discovery cohort, the humanized peptide classifier was able to differentiate between non-diabetic and DN mice (Fig. 3A). The classifier could also significantly discriminate between RASi treated and untreated DN mice (Fig. 3A). This humanized readout was next tested to validate its accuracy in diagnosing disease and detecting drug treatment changes in both an independent cohort of mice and humans.

### **Validation of the humanized urinary peptide based classifier in an independent set of T2D nephropathy mice.**

We further validated the classifier using the additional independent cohort of non-diabetic (n=7), untreated DN (n=10) and RASi-treated DN mice (n=10) (Table 2). In this separate validation set, significant differences were seen not only between non-diabetic and DN animals, but also between untreated DN mice and DN mice treated with RASi (Fig. 3B).

As the aim of the classifier was prediction of DN and not T2D *per se*, we assessed the association of the humanized classifier with the development of glomerular lesions in the

validation cohort. The classifier was highly correlated with glomerular PAS-positive matrix accumulation ( $r=0.6420$ ,  $p=0.0003$ , Fig. 3C) and outperformed albuminuria, the standard readout, that showed a weaker association with renal lesions ( $r=0.4839$ ,  $p=0.0105$ , Fig. 3D). This result supports the hypothesis that multimolecular humanized readouts can better describe complex disease phenotypes<sup>9</sup> than individual biomarkers such as albuminuria routinely used as a biomarker of DN in man.

### **Validation of the humanized urinary peptide based classifier in humans.**

Since the CKD273 classifier was based on 273 urine peptides of human origin, we verified that the selected reduced subset of mouse ortholog peptides used for the humanized urine peptide classifier could efficiently translate to the clinic and predict the presence of DN and respond to RASi treatment in humans. Using a discovery cohort of 25 non-diabetic healthy controls and 25 patients with DN available in the human urinary peptide database<sup>35</sup> (Table 3), we built a classifier based on the orthologs, which significantly distinguished between the 2 groups in the discovery set (Fig. 4A). For a first independent validation of the classifier we scored a small cohort of 42 T2D patients with or without DN, treated either with placebo or with irbesartan, an angiotensin II receptor antagonist representing another class of RASi. In this additional independent validation cohort, the ortholog-based classifier was able to discriminate T2D patients with DN treated with placebo or the RASi (Fig. 4B). As expected, a significant difference was also observed between T2D-patients with and without DN (Fig. 4B). We further validated the classifier using a previously published cohort<sup>27</sup> of 165 T2D patients among which 87 displayed DN as defined by macroalbuminuria and/or eGFR  $<45$  mL/min/1.73 m<sup>2</sup><sup>27</sup>. By this

design, macroalbuminuria and eGFR were strongly associated to the presence of DN (AUC of 0.94 and 0.88 for albuminuria and eGFR, respectively). Patient treatment information was not available in this study <sup>27</sup>. The humanized classifier clearly separated the 165 T2D-patients with and without DN, although with lower sensitivity and specificity than the original CKD273 classifier (AUC of 0.73 and 0.95 for the humanized- and CKD273-classifier, respectively) (Fig. 4C).

## DISCUSSION

The limited success rate of cross-species translation of results from preclinical models to the patient still hampers the pharmaceutical development for many complex diseases including DN. One major hurdle appears that disease progression and therapeutic effects are not adequately captured by animal models <sup>5</sup>. Moreover, readouts used in preclinical studies are usually different from the required endpoints in clinical trials <sup>7</sup>. In animals, the readouts are designed to give the highest discriminative power between healthy and diseased animal, e.g., rely on tissue examination at termination of the study. In contrast, treatment efficiency assessed in clinical trials is often limited to the use of a non- or minimally invasive approach, especially in chronic diseases where biomarkers are used to follow disease progression. This limitation can be exemplified in the DN area, where phase II studies largely depend on changes in albuminuria, which cannot always predict progression of renal lesions or drug treatment benefits.

Here, using urinary peptidomics, we have developed and demonstrated the validity of a non-invasive, humanized multimarker readout of DN. This classifier was shown to correlate with the renal lesions in two prototypic T2D-DN mouse models and also shown to respond to RASi treatment in both mouse models and in a cohort of diabetic patients. Therefore, the classifier tool defined holds great potential for building the translational bridge between a drug candidate's effects in a mouse DN model to human disease. Although we developed this approach for urinary peptides, this concept can, in theory, be applied to any non- or minimal-invasive biological trait including miRNAs, mRNAs, proteins or metabolites. However the availability of reference panels for human disease is a prerequisite.

Reliable markers of DN are needed to characterize the severity of disease and to monitor drug treatment effects in improving kidney health and function. RASi are drugs routinely used to slow-down the progression of DN following the landmark study by Lewis et al. in 1993<sup>36</sup>. Therefore, we decided to use RASi to validate our strategy that drugs that are effective in humans will lead to a positive humanized urinary peptidome readout in selected mouse models, and *vice versa*. We observed that the treatment with RASi (enalapril) moderately, but significantly, reduced the score of the humanized urinary peptide classifier, and that reduced histopathological lesions accompanied the lower scores. In addition, the classifier score was lower in humans with DN treated with irbesartan, an angiotensin II receptor antagonist that represents another class of RASi, validating not only the translational value of the classifier, but also its sensitivity to different drugs from the same class.

Our results strengthen the notion that urine is a rich source of biomarkers and support the hypothesis that multi-peptide panels/readouts can better describe complex disease phenotypes<sup>8, 9</sup>. This is further exemplified by the observation that this novel humanized urine peptide classifier based on 21 urinary peptides displayed a strong and highly significant correlation with lesions *in-situ*, whereas the correlation and significance of albuminuria alone with the score of glomerular lesions in mice, routinely used as a biomarker of DN in man, were much lower. These results are in accordance with previous observations that albuminuria does not always correlates with disease progression in man<sup>37-39</sup>, while multimarker urinary peptidome classifiers have been suggested to better depict disease progression<sup>28, 31, 40</sup>.

The use of body fluid-based humanized classifiers also has the benefit of being non-invasive and would permit longitudinal follow-up and *on-route* adjustment during the drug evaluation

process; no animal sacrifice is needed. Furthermore, such non-invasive assessment of progression of disease in animals will also more closely mimic the surrogate endpoints in human clinical trials where evaluation of renal lesions using kidney biopsies, especially in DN, is not routinely performed. In addition, the option to sample multiple times from the same animal will significantly reduce the number of animals required for long-term studies.

Although our model is based upon multiple markers, all markers in the model were derived from fragments of either collagen  $\alpha$ -1(I) or (III). This can be considered as a limitation as to the concept of a multimarker panel to represent multiple disease mechanisms in complex diseases. Indeed the collagen-based urinary markers most likely represent the development of fibrosis<sup>41</sup> that is considered a hallmark of kidney disease<sup>42,43</sup>. When taking into account the non-ortholog peptides, some of the corresponding proteins could also be linked to human chronic kidney disease or diabetic nephropathy. These include pro-epidermal growth factor<sup>44</sup>, uromodulin<sup>45</sup>, meprin A<sup>46</sup>, osteopontin<sup>47</sup>, complement factor D<sup>48</sup> and  $\alpha$ -1-antitrypsin<sup>49</sup> (Supplementary Table 5). Improvement of the applied strategy will come from new sequence information on the disease-associated peptides in both mice and humans. Updated orthology models based on larger panels of different peptides (i.e. not only composed of collagen I and III fragments) are anticipated to be more resistant to variability, provide an optimized description of molecular mechanisms of disease and hence to improve the confidence in prediction of disease progression and treatment effects. Finally, a validated humanized urine peptide classifier may also facilitate decision making about the preclinical model to use for a specific human disease. In this context it could add to a recent transcriptomics studies<sup>50</sup> using renal tissue that identified cross-species shared transcriptional networks of DN allowing identification of

pathways unique to each of the human-mouse strain networks. Such approaches could reduce the number of different animal models currently used for drug discovery today.

In conclusion we have developed, based on a new concept, the first humanized non-invasive multi-peptide classifier that could provide a step change in translational drug discovery research in T2D-DN.

## **RESEARCH DESIGN AND METHODS**

### **Animals and experimental design**

Male diabetic db/db mice (BKS.Cg-Dock7m +/+ Leprdb/J stock no. 000642) and female BTBRob/ob mice (BTBR.V(B6)-Lepob/WiscJ stock no. 004824) and their respective lean littermates db/m and BTBR were purchased from the Jackson Laboratory (Bar Harbor, ME, USA). All mice had free access to food and water and were maintained on a 12-h light/dark cycle at 21-22°C. Db/m and db/db mice were subjected to right side uninephrectomy (UNx) under anesthesia at 8 weeks of age to accelerate development of diabetic nephropathy as described previously<sup>51</sup>. The following groups of mice were studied: (i) untreated BTBRob/ob diabetic mice (n=9); (ii) BTBRob/ob diabetic mice treated with enalapril (Sigma E6888-5G) admixed in drinking water 200 mg/l with a non-caloric sweetener (Splenda, 240mg/l) for 12 weeks from age 8 to 20 weeks (n=9); (iii) untreated BTBR non-diabetic lean mice (n=9); (iv) untreated UNxdb/db diabetic mice (n=11); (v) UNxdb/db diabetic mice treated with enalapril for 4 weeks from age 18 to 22 weeks (n=9); (vi) untreated UNxdb/m non-diabetic lean mice (n=8). Mice were sacrificed under isoflurane anesthesia at 20 weeks of age in BTBRob/ob and at 22 weeks of age in UNxdb/db. Kidneys were collected for histologic analyses. The experimental protocols were approved by the Animal Care Committee at the University of Utah (UNxdb/db) and the Local Ethics Review Committee on Animal Experiments in the Göteborg Region (BTBRob/ob).

### **Blood and urine chemistry**



Blood glucose and HbA1c levels were measured in fasted awake mice using an Accu-Chek (Roche, REF 05599415370; BTBRob/ob) or a glucose meter (Glucometer Elite XL, Bayer Healthcare, Elkhart, IN, USA; UNxdb/db) and HbA1cNow+ (Bayer, REF 81611409-3038; BTBRob/ob) or DC 2000+ HbA1C kit (Bayer Healthcare; UNxdb/db). To determine albumin excretion rates (AER,  $\mu\text{g}/24\text{ h}$ ) urine was collected from metabolic cages. During urine collection mice had free access to food and water. Urine albumin concentration was measured using a mouse specific albumin ELISA (ICL, E-90AL; BTBRob/ob) or a laser nephelometer (Hyland, Deerfield, Illinois; UNxdb/db) using a monospecific antibody to rat serum albumin (Cappel Laboratories, West Chester, Pennsylvania).

### **Histological analysis**

Kidneys were fixed in Carnoy solution, dehydrated in alcohol, and embedded in paraffin. Two-micrometer sections were stained with periodic acid-Schiff reagent. At least 50 glomeruli, including superficial and juxtaglomerular cortical area, were examined for each animal. The extent of glomerular damage was expressed as the percentage of glomerular area fraction occupied by PAS-positive matrix<sup>51</sup>.

### **Urine peptidomics**

*Sample preparation:* Thirteen hour-urine obtained from BTBRob/ob mice at 20 weeks age and bladder urine collected from UNxdb/db mice at 22 weeks age at termination were used for peptide profiling, respectively. One hundred fifty  $\mu\text{l}$  of mouse urine sample was diluted with the same volume of a solution composed of 2 M urea, 10 mM  $\text{NH}_4\text{OH}$  and 0.2% SDS. Subsequently,

samples were ultrafiltered using a Centrstat 20 kDa cut-off centrifugal filter device (Satorius, Göttingen, Germany) to eliminate high molecular weight molecules. The filtrate was desalted using a NAP5 gel filtration column (GE Healthcare Bio Sciences, Uppsala, Sweden) to remove urea and electrolytes, and thereby to decrease matrix effects. The sample was lyophilized in a Savant speedvac SVC100H connected to a Virtis 3L Sentry freeze dryer (Fischer Scientific, Illkirch, France) and stored at 4°C until use. Shortly before CE-MS analysis, the samples were re-suspended in 10µL HPLC grade H<sub>2</sub>O.

*CE-MS Analysis:* CE-MS analysis was performed as previously described<sup>52, 53</sup>. Briefly, CE-MS analyses were performed using a Beckman Coulter Proteome Lab PA800 capillary electrophoresis system (Beckman Coulter, Fullerton, USA) on-line coupled to a micrOTOF II MS (Bruker Daltonic, Bremen, Germany). The electro-ionization sprayer (Agilent Technologies, Palo Alto, CA, USA) was grounded, and the ion spray interface potential was set to -4.5 kV. Data acquisition and MS acquisition methods were automatically controlled by the CE via contact-close-relays. Spectra were accumulated every 3 s, over a range of  $m/z$  350 to 3000.

*Data Processing and Cluster Analysis:* MosaiquesVisu software package was applied to deconvolve mass spectral ion peaks representing identical molecules at different charge states into single masses<sup>54</sup>. Migration time and ion signal intensity (amplitude) were normalized using internal polypeptide standards<sup>55</sup>. Each polypeptide present in the list was defined by its normalized migration time [min], molecular mass [kDa], and signal intensity detected. Using a Microsoft SQL database, all detected polypeptides were deposited, matched, and annotated in order to allow for further comparison between the groups. The criteria applied to considered a polypeptide identical was that within different samples the mass deviation was lower than 50

ppm for masses <4kDa, 150 ppm for masses >6kDa, and between 50-150 ppm for masses between 4-6kDa. Acceptable migration time deviation was between 1 and 2.5 minutes.

*Peptide sequencing:* For sequencing, processed urine samples were also separated on a Dionex Ultimate 3000 RSLC nano flow system (Dionex, Camberly UK). A 5  $\mu$ l sample was loaded onto a Dionex 5 mm C18 nano trap column at a flowrate of 5  $\mu$ l/min. Elution was performed on an Acclaim PepMap 75 mm C18 nano column over 100 min. The sample was ionised in positive ion mode using a Proxeon nano spray ESI source (Thermo Fisher Hemel UK) and analyzed in an Orbitrap Velos FTMS (Thermo Finnigan, Bremen, Germany). The MS was operated in data-dependent mode to switch between MS and MS/MS acquisition and parent ions were fragmented by (high-) energy collision-induced dissociation and also electron transfer dissociation. Data files were searched against *Mus musculus* entries in the Swiss-Prot database without any enzyme specificity using Open Mass Spectrometry Search Algorithm (OMSSA, <http://pubchem.ncbi.nlm.nih.gov/omssa>) with an e-value cut-off of 0.1. No fixed modification and oxidation of methionine as variable modifications were selected. Mass error windows of 10 ppm for MS and 0.05 Da (HCD) or 0.5 Da (CID, ETD) for MS/MS were allowed. For further validation of obtained peptide identifications, the strict correlation between peptide charge at pH 2 and CE-migration time was utilized to minimize false-positive identification rates<sup>56</sup>. Calculated CE-migration time of the sequence candidate based on its peptide sequence (number of basic amino acids) was compared to the experimental migration time. Peptides were accepted only if they had a mass deviation below  $\pm$  80 ppm and a CE-migration time deviations below  $\pm$  2 min.

### **Human data CE-MS and patient data**

Human CE-MS data and general patient characteristics (Table 5) were extracted from the human urinary peptide database<sup>35</sup> and from<sup>27</sup>. The study was designed and conducted fulfilling all of the requisites of the laws on the protection of individuals collaborating in medical research and was in accordance with the principles of the Declaration of Helsinki. All datasets included in the study derived from previous studies and all data were anonymized. The approach employing anonymized proteomics data from previous studies was approved by the local ethics committee.

### **Orthology**

To examine the orthology between mouse peptides and human peptides from CKD273<sup>24</sup> we applied three criteria: first, we looked for identical fragments; secondly, we looked for fragments with one identical cleavage site (N or C-term) and third, we looked for peptides from the same protein area with a minimum overlap in 6 amino acids.

### **Statistics**

*Comparisons and correlations:* Statistical comparisons between two groups were assessed using a Mann-Whitney test for independent samples. Correlations were assessed using a non-parametric Spearman correlation test. All statistics were performed using the Prism 5 GraphPad software.

*Biomarker selection and classifier modelling:* For the identification of potential biomarkers, the reported p-values were calculated using the Wilcoxon Rank-Sum test (R-based statistic software, version 2.15.3) followed by adjustment for multiple testing using the method described by Benjamini and Hochberg <sup>57</sup>. Peptides that were detectable in >70% of mice in at least one group and reached an adjusted p-value of <0.05 were further considered as relevant. Using MosaCluster software package <sup>52</sup> we next used a support vector machine (SVM)-based approach <sup>58</sup> to generate a prognostic biomarker classifier based on 21 mice ortholog biomarkers associated with DN and that were sequenced. The parameters of the kernel function for the 21-dimensional hyperplane were: penalty parameter (C) of 4 and kernel width ( $\gamma$ ) of 0.00819. The ortholog-based human model was formed by 19 biomarkers and the parameters used for the hyperplane were: penalty parameter (C) of 1024 and kernel width ( $\gamma$ ) of 0.00012. Sensitivity and specificity were calculated based on the number of properly classified samples. The overall yield of the polypeptide pattern was evaluated by the receiver operating characteristic (ROC) and area under curve (AUC) plots with MedCalc software (MedCalc version 8.1.1.0, MedCalc Software, Belgium).

## **DISCLOSURE**

AE and XRP are employees of Astra-Zeneca. JS and ART are/were employees of Mosaiques Diagnostics GmbH. HM is cofounder and a shareholder of Mosaiques Diagnostics GmbH.

## REFERENCES

1. Eckardt KU, Coresh J, Devuyst O, et al. Evolving importance of kidney disease: from subspecialty to global health burden. *Lancet*. 2013;382:158-169.
2. Afkarian M, Sachs MC, Kestenbaum B, et al. Kidney disease and increased mortality risk in type 2 diabetes. *J Am Soc Nephrol*. 2013;24:302-308.
3. Himmelfarb J, Tuttle KR. New therapies for diabetic kidney disease. *N Engl J Med*. 2013;369:2549-2550.
4. Zoja C, Zanchi C, Benigni A. Key pathways in renal disease progression of experimental diabetes. *Nephrol Dial Transplant*. 2015;30 Suppl 4:iv54-59.
5. Ioannidis JP. Extrapolating from animals to humans. *Science translational medicine*. 2012;4:151ps115.
6. Hartung T. Look back in anger - what clinical studies tell us about preclinical work. *Altex*. 2013;30:275-291.
7. Denayer T, Stöhr T, Van Roy M. Animal models in translational medicine: Validation and prediction. *New Horizons in Translational Medicine*. 2014;2:5-11.
8. Hurst RE. Does the biomarker search paradigm need re-booting? *BMC Urol*. 2009;9:1.
9. Rifai N, Gillette MA, Carr SA. Protein biomarker discovery and validation: the long and uncertain path to clinical utility. *Nature biotechnology*. 2006;24:971-983.
10. Ito R, Takahashi T, Katano I, et al. Current advances in humanized mouse models. *Cellular & molecular immunology*. 2012;9:208-214.
11. Tesch GH, Lim AK. Recent insights into diabetic renal injury from the db/db mouse model of type 2 diabetic nephropathy. *American journal of physiology Renal physiology*. 2011;300:F301-310.
12. Hudkins KL, Pichaiwong W, Wietecha T, et al. BTBR Ob/Ob mutant mice model progressive diabetic nephropathy. *J Am Soc Nephrol*. 2010;21:1533-1542.
13. Pichaiwong W, Hudkins KL, Wietecha T, et al. Reversibility of structural and functional damage in a model of advanced diabetic nephropathy. *J Am Soc Nephrol*. 2013;24:1088-1102.

14. Zhou G, Cheung AK, Liu X, et al. Valsartan slows the progression of diabetic nephropathy in db/db mice via a reduction in podocyte injury, and renal oxidative stress and inflammation. *Clinical science*. 2014;126:707-720.
15. Eisner C, Faulhaber-Walter R, Wang Y, et al. Major contribution of tubular secretion to creatinine clearance in mice. *Kidney Int*. 2010;77:519-526.
16. Bivona BJ, Park S, Harrison-Bernard LM. Glomerular filtration rate determinations in conscious type II diabetic mice. *American journal of physiology Renal physiology*. 2011;300:F618-625.
17. Mischak H, Delles C, Vlahou A, et al. Proteomic biomarkers in kidney disease: issues in development and implementation. *Nature reviews Nephrology*. 2015;11:221-232.
18. Schanstra JP, Mischak H. Proteomic urinary biomarker approach in renal disease: from discovery to implementation. *Pediatr Nephrol*. 2015;30:713-725.
19. Klein J, Bascands JL, Mischak H, et al. The role of urinary peptidomics in kidney disease research. *Kidney Int*. 2016;89:539-545.
20. Klein J, Lacroix C, Caubet C, et al. Fetal Urinary Peptides to Predict Postnatal Outcome of Renal Disease in Fetuses with Posterior Urethral Valves (PUV). *Science translational medicine*. 2013;5.
21. Zimmerli LU, Schiffer E, Zurbig P, et al. Urinary proteomic biomarkers in coronary artery disease. *Mol Cell Proteomics*. 2008;7:290-298.
22. Weissinger EM, Metzger J, Dobbstein C, et al. Proteomic peptide profiling for preemptive diagnosis of acute graft-versus-host disease after allogeneic stem cell transplantation. *Leukemia*. 2013.
23. Metzger J, Negm AA, Plentz RR, et al. Urine proteomic analysis differentiates cholangiocarcinoma from primary sclerosing cholangitis and other benign biliary disorders. *Gut*. 2013;62:122-130.
24. Good DM, Zurbig P, Argiles A, et al. Naturally occurring human urinary peptides for use in diagnosis of chronic kidney disease. *Mol Cell Proteomics*. 2010;9:2434-2437.
25. Andersen S, Mischak H, Zuerbig P, et al. Urinary proteome analysis enables assessment of renoprotective treatment in type 2 diabetic patients with microalbuminuria. *BMC nephrology*. 2010;11.

26. Molin L, Seraglia R, Lapolla A, et al. A comparison between MALDI-MS and CE-MS data for biomarker assessment in chronic kidney diseases. *Journal of proteomics*. 2012;75:5888-5897.
27. Siwy J, Schanstra JP, Argiles A, et al. Multicentre prospective validation of a urinary peptidome-based classifier for the diagnosis of type 2 diabetic nephropathy. *Nephrology Dialysis Transplantation*. 2014;29:1563-1570.
28. Schanstra JP, Zurbig P, Alkhalaf A, et al. Diagnosis and Prediction of CKD Progression by Assessment of Urinary Peptides. *J Am Soc Nephrol*. 2015;26:1999-2010.
29. Argiles A, Siwy J, Duranton F, et al. CKD273, a new proteomics classifier assessing CKD and its prognosis. *PloS one*. 2013;8:e62837.
30. Roscioni SS, de Zeeuw D, Hellemons ME, et al. A urinary peptide biomarker set predicts worsening of albuminuria in type 2 diabetes mellitus. *Diabetologia*. 2013;56:259-267.
31. Zurbig P, Jerums G, Hovind P, et al. Urinary proteomics for early diagnosis in diabetic nephropathy. *Diabetes*. 2012;61:3304-3313.
32. Rossing K, Mischak H, Rossing P, et al. The urinary proteome in diabetes and diabetes-associated complications: New ways to assess disease progression and evaluate therapy. *Proteomics Clin Appl*. 2008;2:997-1007.
33. Siwy J, Zoja C, Klein J, et al. Evaluation of the Zucker diabetic fatty (ZDF) rat as a model for human disease based on urinary peptidomic profiles. *PloS one*. 2012;7:e51334.
34. Zhong Y, Chen EY, Liu R, et al. Renoprotective effect of combined inhibition of angiotensin-converting enzyme and histone deacetylase. *J Am Soc Nephrol*. 2013;24:801-811.
35. Siwy J, Mullen W, Golovko I, et al. Human urinary peptide database for multiple disease biomarker discovery. *Proteomics Clin Appl*. 2011;5:367-374.
36. Lewis EJ, Hunsicker LG, Bain RP, et al. The effect of angiotensin-converting-enzyme inhibition on diabetic nephropathy. The Collaborative Study Group. *N Engl J Med*. 1993;329:1456-1462.
37. Miller WG, Bruns DE, Hortin GL, et al. Current issues in measurement and reporting of urinary albumin excretion. *Clin Chem*. 2009;55:24-38.
38. Maclsaac RJ, Ekinci EI, Jerums G. 'Progressive diabetic nephropathy. How useful is microalbuminuria?: contra'. *Kidney Int*. 2014;86:50-57.



39. Perkins BA, Ficociello LH, Roshan B, et al. In patients with type 1 diabetes and new-onset microalbuminuria the development of advanced chronic kidney disease may not require progression to proteinuria. *Kidney Int.* 2010;77:57-64.
40. Pontillo C, Jacobs L, Staessen JA, et al. A urinary proteome-based classifier for the early detection of decline in glomerular filtration. *Nephrol Dial Transplant.* 2016;in press.
41. Mischak H, Delles C, Klein J, et al. Urinary proteomics based on capillary electrophoresis-coupled mass spectrometry in kidney disease: discovery and validation of biomarkers, and clinical application. *Advances in chronic kidney disease.* 2010;17:493-506.
42. Eddy AA, Neilson EG. Chronic kidney disease progression. *J Am Soc Nephrol.* 2006;17:2964-2966.
43. Liu Y. Cellular and molecular mechanisms of renal fibrosis. *Nature reviews Nephrology.* 2011;7:684-696.
44. Klein J, Bascands JL, Buffin-Meyer B, et al. Epidermal growth factor and kidney disease: a long-lasting story. *Kidney Int.* 2016;89:1125-1135.
45. Eddy AA. Scraping fibrosis: UMODulating renal fibrosis. *Nat Med.* 2011;17:553-555.
46. DeGuzman JB, Speiser PW, Trachtman H. Urinary meprin-alpha: a potential marker of diabetic nephropathy. *J Pediatr Endocrinol Metab.* 2004;17:1663-1666.
47. Al-Malki AL. Assessment of urinary osteopontin in association with podocyte for early prediction of nephropathy in diabetic patients. *Disease markers.* 2014;2014:493736.
48. Fearn A, Sheerin NS. Complement activation in progressive renal disease. *World J Nephrol.* 2015;4:31-40.
49. Smith A, L'Imperio V, De Sio G, et al. alpha-1-antitrypsin detected by MALDI-Imaging in the study of glomerulonephritis: its relevance in chronic kidney disease progression. *Proteomics.* 2016.
50. Hodgin JB, Nair V, Zhang H, et al. Identification of cross-species shared transcriptional networks of diabetic nephropathy in human and mouse glomeruli. *Diabetes.* 2013;62:299-308.
51. Huang Y, Border WA, Yu L, et al. A PAI-1 mutant, PAI-1R, slows progression of diabetic nephropathy. *J Am Soc Nephrol.* 2008;19:329-338.

52. Decramer S, Wittke S, Mischak H, et al. Predicting the clinical outcome of congenital unilateral ureteropelvic junction obstruction in newborn by urinary proteome analysis. *Nat Med.* 2006;12:398-400.
53. Mischak H, Vlahou A, Ioannidis JP. Technical aspects and inter-laboratory variability in native peptide profiling: the CE-MS experience. *Clinical biochemistry.* 2013;46:432-443.
54. Neuhoff N, Kaiser T, Wittke S, et al. Mass spectrometry for the detection of differentially expressed proteins: a comparison of surface-enhanced laser desorption/ionization and capillary electrophoresis/mass spectrometry. *Rapid Commun Mass Spectrom.* 2004;18:149-156.
55. Dissard R, Klein J, Caubet C, et al. Long term metabolic syndrome induced by a high fat high fructose diet leads to minimal renal injury in C57BL/6 mice. *PloS one.* 2013;8:e76703.
56. Züribig P, Renfrow MB, Schiffer E, et al. Biomarker discovery by CE-MS enables sequence analysis via MS/MS with platform-independent separation. *Electrophoresis.* 2006;27:2111-2125.
57. Benjamini Y, Hochberg Y. Controlling the false discovery rate: a practical and powerful approach to multiple testing. *Journal of the Royal Statistical Society (Series B: Methodological).* 1995;57:289-300.
58. Weissinger EM, Wittke S, Kaiser T, et al. Proteomic patterns established with capillary electrophoresis and mass spectrometry for diagnostic purposes. *Kidney Int.* 2004;65:2426-2434.

## **ACKNOWLEDGMENTS**

We are grateful to Pernilla Håkansson for performing the BTBRob/ob experimental work and to Ulrika Johansson for facilitating the UNxdb/db studies. Gerhard Böttcher and Ann-Katrin Andersson for assisting with histopathology. This work was supported in part by the « Fondation du Rein sous égide de la Fondation pour la Recherche Médicale et ses partenaires », grant number GENZYME 2014 FDR-SdN/FRM for JK.

## FIGURE LEGENDS

Fig. 1. Improving the translatability of animal models of disease by the development of a multimolecular humanized readout. *A*: Disease readouts are often based on a single phenotypic trait or biomarker similar, if possible, in animals and humans. Such single feature does not capture the complexity of most disorders. Hence novel drugs, although successful in the preclinical phase based on such single feature readout in animal models, often fail in humans. *B*: In contrast, the analysis of multimolecular changes using omics approaches, by for example urinary peptidomics, allows a more complete description of complex phenotypes. Furthermore the combination of these multiple features similar (ortholog) in human disease and animal models, leading to a “humanized” readout, most likely will more efficiently translate the effects of new drugs in preclinical models to the clinic.

Fig. 2. The biological response, histology and urinary peptidome are highly comparable in two frequently used T2D nephropathy mouse strains. *A*: albumin excretion rate, *B*: glomerular periodic acid Schiff staining -positive matrix fraction and *C*: representative histology sections of glomerular mesangial matrix deposition stained with periodic acid Schiff staining; Scale bars: 100µm. *D*: Representation of urinary peptides significantly modified between non-diabetic and mice with DN. Each peptide is identified using CE-MS by a unique identifier on the basis of the migration time (min) and specific mass (kDa), with a peak height representing the relative abundance. *E* and *F*: Venn diagrams showing the overlap of urinary peptides significantly modified in the two T2D mouse strains with DN and overlap in response to RASi. BTBRob/ob, T2D mice with leptin-deficiency mutation; Unxdb/db uninephrectomized T2D mice with a

mutation in the leptin receptor; No diab, lean control mice; DN, T2D mice with diabetic nephropathy; DN+RASi, T2D mice with diabetic nephropathy treated with inhibitors of the renin angiotensin system (RASi, enalapril); PAS<sup>+</sup>, periodic acid Schiff positive; AER, urinary albumin excretion rate. \*p<0.05 versus No diab. °p<0.05 versus non treated DN. Mann-Whitney test for independent samples. Data presented as mean ± SEM.

Fig. 3. Development and validation of a humanized urinary peptide based classifier in T2D nephropathy mice. *A*: scores of the humanized classifier in the discovery cohort consisting of 10 non-diabetic, 10 untreated diabetic and 8 diabetic mice treated with RASi and in the validation cohort *B*: consisting of 7 non-diabetic, 10 untreated diabetic and 10 RASi-treated diabetic mice. *C-D*: Correlation of the humanized urine peptide classifier score (*C*) and albumin excretion rate (*D*) with the glomerular mesangial matrix deposition assessed by periodic acid Schiff staining using the Spearman correlation test. No. diab, lean control mice; DN, T2D mice with diabetic nephropathy; RASi: enalapril; PAS<sup>+</sup>, periodic acid Schiff positive; AER, urinary albumin excretion rate; BTBRob/ob, type 2 diabetic mice; UNxdb/db mice, type 2 diabetic mice. \*p<0.05 versus No diab. °p<0.05 versus DN. Mann-Whitney test for independent samples. Data presented as mean ± SEM.

Fig. 4. Validation of the humanized urinary peptide based classifier in humans. *A*: Scores of the humanized urine peptide classifier in a discovery human cohort consisting of 25 healthy controls and 25 patients with T2D and DN. *B*: Scores of the humanized urine peptide classifier in a validation cohort consisting of 14 patients with T2D without DN, 14 patients with DN treated

with placebo and 14 patients with DN treated with RASi. C: Score, AUC, sensitivity and specificity of the humanized urine peptide classifier and the CKD273 classifier in a supplementary human cohort consisting of 165 T2D-patients with (n=87) and without DN (n=78), for patient details see <sup>27</sup>. No. diab, healthy humans; DN, diabetic humans with diabetic nephropathy; Diab. noDN, diabetic humans without diabetic nephropathy; RASi: irbesartan; Pla, placebo; AUC, area under the curve. \*p<0.05 versus No diab. or Diab. noDN. °p<0.05 versus DN+Pla. Mann-Whitney test for independent samples. Data presented as mean ± SEM.

## TABLES

**Table 1. Blood chemistry data of BTBRob/ob and UNxdb/db mice.**

	BTBR			Unxdb		
	No diab. (BTBR)	DN (BTBRob/ob)	DN+RASi	No diab. (Unxdb/m)	DN (Unxdb/db)	DN+RASi
<b>Glucose (mM)</b>	9.1 ±0.2	24.3 ±2.8*	26.3 ±2.9*	5.7 ±0.5	33.3 ±4.7*	33.3 ±0.0*
<b>HbA1c (%) [mmol/mol]</b>	4.7 ±0.1 [28 ±1]	11.5 ±0.4 [103 ±4]*	11.5 ±0.4 [102 ±4]*	4.0 ±0.1 [20 ±1]	13.3 ±0.4 [123 ±4]*	13.4 ±0.4 [123 ±5]*

Data presented as mean ± SEM (n=5-11/ group). BTBRob/ob, T2D mice with leptin-deficiency mutation; Unxdb/db uninephrectomized T2D mice with a mutation in the leptin receptor; No diab., lean control mice; DN, T2D mice with diabetic nephropathy; DN+RASi, T2D mice with diabetic nephropathy treated with inhibitors of the renin angiotensin system (RASi, enalapril); HbA1c, glycated haemoglobin A1c. \*p<0.05 versus No diab. Mann-Whitney test for independent samples.

**Table 2. Biochemistry data of mouse discovery and validation cohorts.**

	Discovery cohort			Validation cohort		
	No diab.	DN	DN+RASi	No diab.	DN	DN+RASi
<b>Number (BTBRob/ob/Unxdb/db)</b>	10 (5/5)	10 (5/5)	8 (4/4)	7 (4/3)	10 (4/6)	10 (5/5)
<b>Albumin excretion rate (mg/24h)</b>	0.03 ±0.01	1.4 ±0.4*	0.4 ±0.11* <sup>o</sup>	0.1 ±0.1	1.1 ±0.3*	0.7 ±0.3*
<b>Glomerular PAS+ (%)</b>	19.6 ±4.0	50.1 ±2.5*	25.5 ±1.4 <sup>o</sup>	14.1 ±1.1	44.5 ±1.2*	32.5 ±3.6* <sup>o</sup>
<b>Blood glucose (mM)</b>	7.2 ±0.7	25.6 ±3.2*	27.3 ±3.0*	7.8 ±0.8	30.6 ±2.1*	31.8 ±1.6*
<b>HbA1c (%) [mmol/mol]</b>	4.4 ±0.1 [24 ±1]	11.8 ±0.5 [105 ±6]*	12.3 ±0.6 [111 ±7]*	4.5 ±0.2 [25 ±2]	12.8 ±0.4 [117 ±4]*	12.5 ±0.5 [114 ±5]*

Data presented as mean ± SEM. No diab., lean control mice; DN, T2D mice with diabetic nephropathy; RASi: enalapril; AER, urinary albumin excretion rate; PAS<sup>+</sup>, periodic acid Schiff positive; HbA1c, glycated haemoglobin A1c; BTBRob/ob, type 2 diabetic mice; UNxdb/db mice, type 2 diabetic mice. \*p<0.05 versus No diab. <sup>o</sup>p<0.05 versus DN. Mann-Whitney test for independent samples.



**Table 3. Biochemistry data of human discovery and validation cohorts.**

	Discovery cohort		Validation cohort			Supplementary cohort	
	No diab.	DN	Diab. noDN	DN+Placebo	DN+RASi	Diab. noDN	DN
<b>Gender</b> (M/F)	20/5	25/0	11/3	14/0	12/2	19/28 (for 31 n.a.)	35/23 (for 29 n.a.)
<b>Age</b> (years)	62.4 ± 4.0	65.1 ± 5.5	63.9 ± 4.7	67.3 ± 4.7	65.4 ± 4.6	58.1 ± 14.2 (for 33 n.a.)	62.6 ± 14.7 (for 28 n.a.)
<b>eGFR</b> (mL/min/1.73m <sup>2</sup> )	75.3 ± 7.5	55.5 ± 4.6*	80.1 ± 5.4	53.1 ± 3.1*	53.9 ± 4.8*	90.1 ± 19.0	47.6 ± 27.6*
<b>HbA1c</b> (%) [mmol/mol]	n.a.	6.5 ± 0.7 [48 ± 2]	7.8 ± 0.9 [63 ± 3]	7.2 ± 0.8 [55 ± 2]	8.5 ± 0.6 [69 ± 2] <sup>°</sup>	n.a.	n.a.
<b>U-Albumin</b>							
mg/mL	2.3 ± 5.3	228.2 ± 241.6 *	41.1 ± 27.7	71.6 ± 76,3		11.8 ± 7.2 (n=28)	994.4 ± 2224.5 (n=32)
mg/g creatinine						6.3 ± 5.8 (n=31)	655.4 ± 714.3 (n=30)
mg/24h					241.0 ± 282.3	7.4 ± 5.7 (n=19)	3682.5 ± 2999.3 (n=10)
<b>U-Protein</b> (mg/24h)							2914.0 ± 2249.9 (n=10)

Data presented as mean ± SEM. No diab., healthy humans; DN, diabetic humans with diabetic nephropathy; Diab. noDN, diabetic humans without diabetic nephropathy; RASi: irbesartan; Pla, placebo; n.a, not available; eGFR, estimated glomerular filtration rate; HbA1c, glycated haemoglobin A1c; U-albumin or U-protein, urinary albumin or urinary protein excretion, respectively. Since data were collected from different cohorts, urinary albumin was measured using different collection-and normalisation-methods. For 5 patients U-albumin or protein was not available. \*p<0.05 versus No diab. or Diab. noDN. <sup>°</sup>p<0.05 versus DN+Pla. Mann-Whitney test for independent samples.

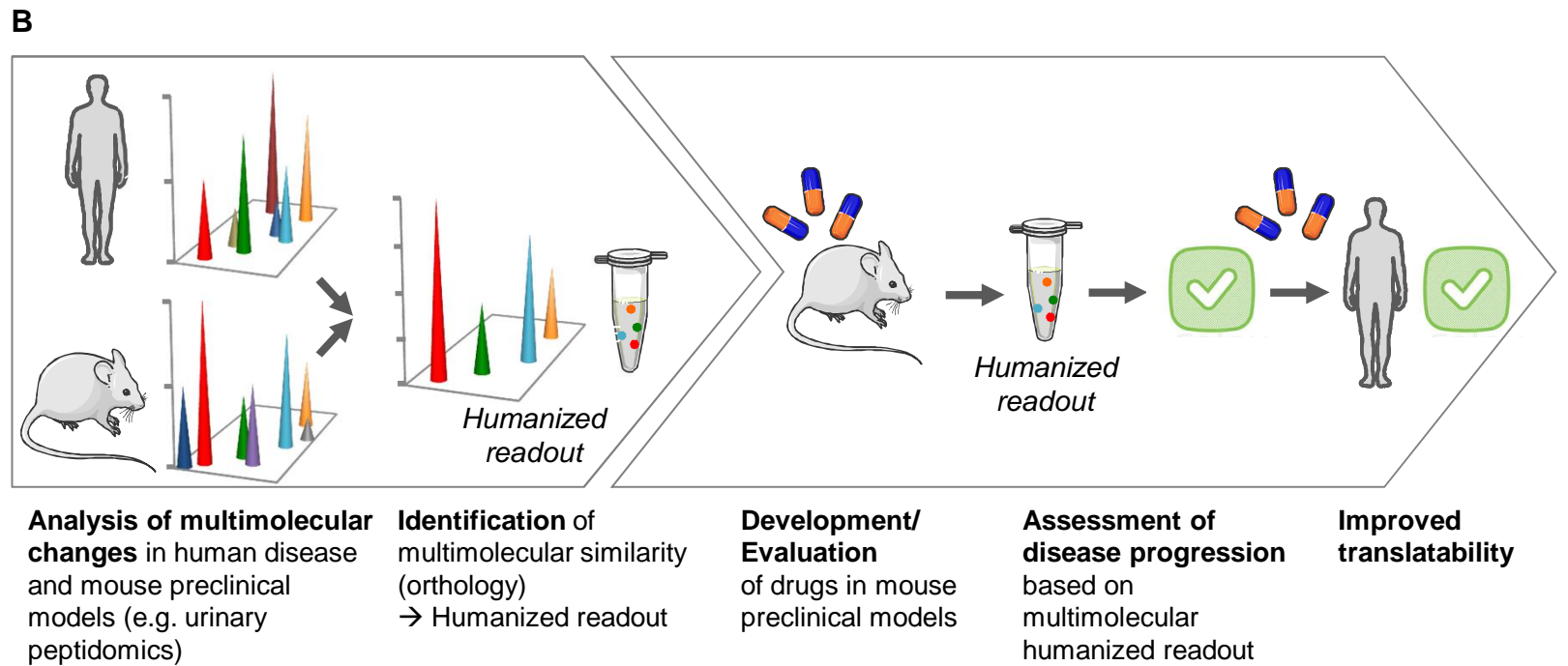
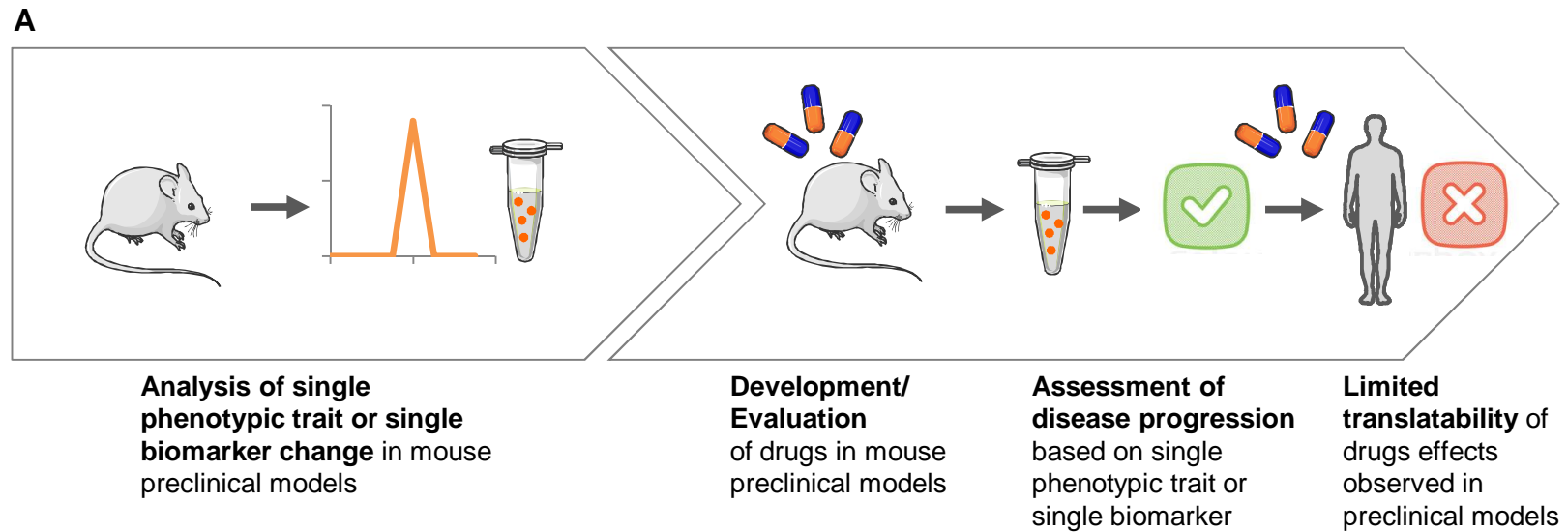


**Figure 1**

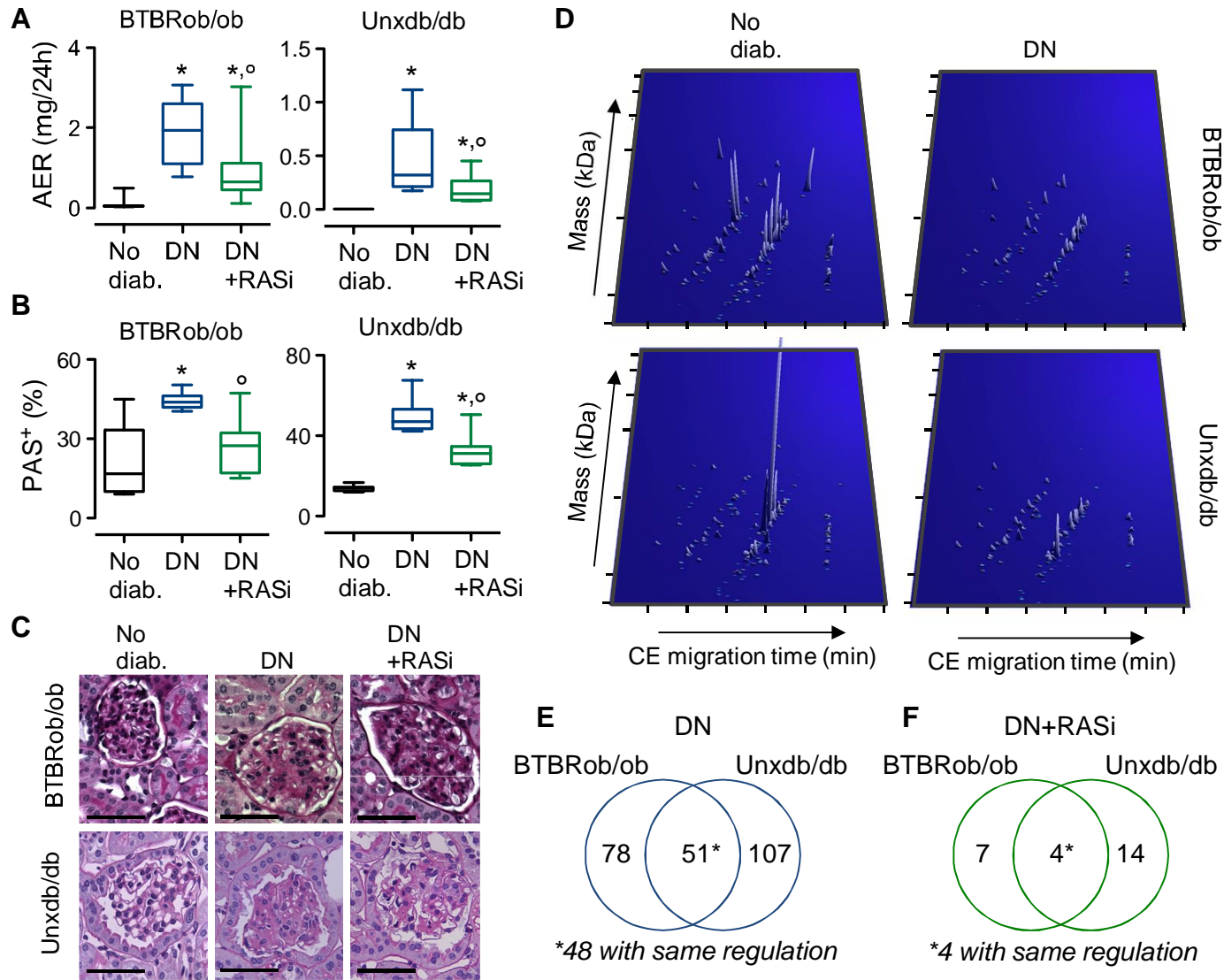


**Figure 2**

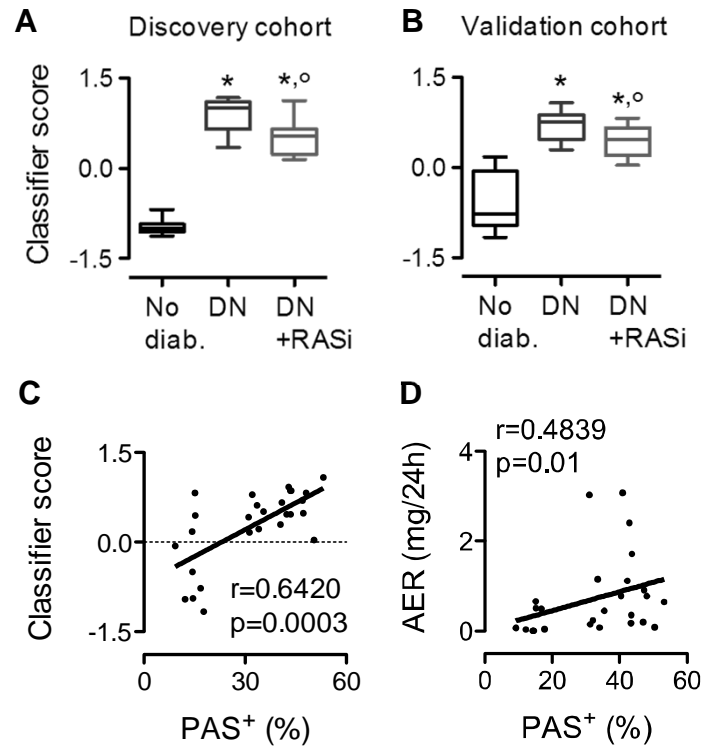
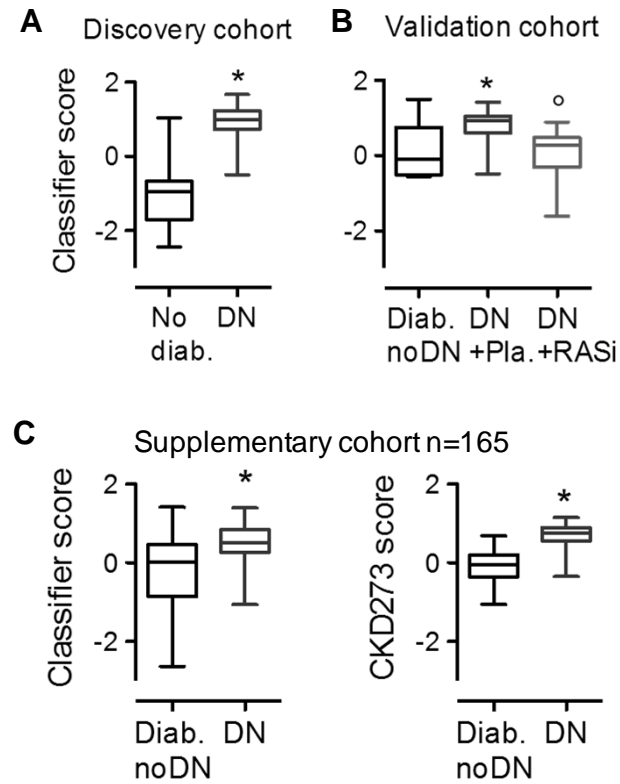


**Figure 3**



	Classifier	CKD273
AUC [CI 95%]	0.729 [0.654-0.795]	0.948 [0.902-0.977]
Sensitivity [CI 95%] (%)	81 [76-92]	90 [81-95]
Specificity [CI 95%] (%)	59 [47-76]	92 [84-97]

**Figure 4**



19285	EVGPPpGpPAGEKGSpG	Collagen alpha-1(i) chain	910	927	P11087	1633.82	41.12	0.003740306	1	8059.6	1	3507.43	0.43518661	down-regulated in ob/ob						
19345	GSgSPGpGKTPpGpPAG	Collagen alpha-1(i) chain	531	549	P11087	1636.83	40.73	0.012479191	1	4111.71	0.89	6559.88	1.595414073	up-regulated in ob/ob						
19367	APFKFKWVDCVS	Complement factor D	88	100	P03953	1637.8	32.93	0.005603303	0.89	694.47	0.11	8.19	0.011793166	down-regulated in ob/ob						
19626	EVGPPpGpGAGEKGSgG	Collagen alpha-1(i) chain	910	927	P11087	1649.81	42.28	0.012479191	1	165.35	1	9453.33	0.271216359	down-regulated in ob/ob						
19814	GLGpGpGAGEKpGGEQ	Collagen alpha-1(i) chain	633	650	P11087	1662.83	41	0.002949087	1	3541.81	1	6708.74	1.894155813	up-regulated in ob/ob						
20085	TGpGpGpGpGAGEKGEA	Collagen alpha-1(i) chain	755	773	P11087	1676.84	41.36	0.004385248	1	1202.25	1	2971.04	2.471233105	up-regulated in ob/ob						
20385	GEVgPpGpGAGEKGSgG	Collagen alpha-1(i) chain	909	927	P11087	1690.83	41.14	0.016072859	0.44	78.84	1	348.68	4.422628108	up-regulated in ob/ob						
20503	YSNKELGNQSIDLL	Kidney androgen-regulated protein	25	39	P61110	1697.99	40.83	0.003740306	1	26893.79	0	0	0	down-regulated in ob/ob						
20763	SPRESASLQSSDRVL	Pro-epidermal growth factor	626	641	P01132	1713.91	34.12	0.012142889	0.78	4136.56	0.11	11.04	0.002668884	down-regulated in ob/ob						
21009	ASHEIATLNGDFALRL	Alpha-1-antitrypsin 1-4	40	55	Q00897	1726.88	34.18	0.02550148	0.33	164.23	0.89	1183.23	7.204712903	up-regulated in ob/ob						
21108	PGGTGAAGTPGKMGPPGPPG	EMI domain-containing protein 1	232	251	Q91VFS	1730.89	39.23	0.039110041	1	1534.05	0.89	939.39	0.612359441	down-regulated in ob/ob						
21455	GTGARGAPDRDGEAGPPGG	Collagen alpha-1(i) chain	781	799	P11087	1747.81	36.04	0.04691826	0.89	171.09	0.22	47.6	0.278216144	down-regulated in ob/ob						
21893	DGGpGAKGpGDTGVKDA	Collagen alpha-1(i) chain	809	827	P11087	1770.89	35.47	0.003485285	1	466.91	1	1073.81	2.299822236	up-regulated in ob/ob						
22065	YLNRSSEGGDGLVGL	Napsin-A	215	231	O09043	1779.88	41.85	0.003740306	1	1575.48	1	2981.4	1.892375657	up-regulated in ob/ob						
22220	DGGpGAKGpGDTGVKDA	Collagen alpha-1(i) chain	809	827	P11087	1786.86	35.6	0.004385248	1	1371.97	1	2276	1.658928402	up-regulated in ob/ob						
22880	VEGEGPSpGpTAGApGTAGP	Collagen alpha-2(i) chain	849	869	Q01149	1824.89	42.14	0.02550148	1	1030.46	1	2207.02	2.14178134	up-regulated in ob/ob						
22917	SPRESASLQSSDRVL	Pro-epidermal growth factor	626	642	P01132	1826.96	35.11	0.004385248	0.89	2980.38	0	0	0	down-regulated in ob/ob						
23042	GpGTGpGpGAGEKpGpG	Collagen alpha-1(iii) chain	641	660	P08121	1834.89	41.58	0.012479191	1	3253.68	0.89	5840.31	1.794985895	up-regulated in ob/ob						
23356	IELSKASDYYRVNVEL	ATP-binding cassette sub-family A member	1292	1307	Q55569	1849.93	34.64	0.012479191	1	965.05	0.89	5251.04	5.4412103	up-regulated in ob/ob						
23770	GpGTGpGpGAGEKGSgG	Collagen alpha-1(iii) chain	764	784	P08121	1875.92	42.43	0.007164724	1	1160.08	0.67	297.86	0.256758155	down-regulated in ob/ob						
24239	ETGAPRpGpGpGpGpGpG	Collagen alpha-1(i) chain	901	921	P11087	1900.94	42.53	0.003740306	1	1750.2	1	4283.88	2.447651697	up-regulated in ob/ob						
24713	ALDpDVESXIFYAQTIA	Pro-epidermal growth factor	522	538	P01132	1929.97	42.48	0.005603303	0.89	6125.23	0.11	18.25	0.00297948	down-regulated in ob/ob						
25110	VVPHPGSRPDSLEDLL	Complement factor D	101	118	P03953	1958.05	35.31	0.004385248	1	2542.72	0.22	31.58	0.00240732	down-regulated in ob/ob						
25169	IGpGTGpGpGpGpGpGpG	Collagen alpha-1(iii) chain	640	660	P08121	1962.95	42.24	0.019906338	1	2370.47	1	3687.96	1.555792733	up-regulated in ob/ob						
25395	RpGpGpGpGpGAGEKGSgG	Collagen alpha-1(i) chain	907	927	P11087	1975.97	35.73	0.004385248	0.89	2080.23	0	0	0	down-regulated in ob/ob						
25689	GPpGpGAGEKpGpGpGAGEK	Collagen alpha-1(i) chain	507	528	P11087	1994.03	29.77	0.012479191	1	919.01	0.89	2294.12	2.496294926	up-regulated in ob/ob						
25768	SNDFIDTRVLNGLPTR	Uromodulin	590	607	Q91X17	2000.1	35.77	0.019906338	1	2732.53	0.56	2810.49	0.102863461	down-regulated in ob/ob						
26052	GRpGpGpGpGpGAGEKGSgG	Collagen alpha-1(i) chain	906	927	P11087	2017.01	35.92	0.007501881	0.89	374.55	0.11	19.79	0.052836737	down-regulated in ob/ob						
26273	GRpGpGpGpGpGAGEKGSgG	Collagen alpha-1(i) chain	906	927	P11087	2033.01	36.09	0.007501881	0.78	168.66	0	0	0	down-regulated in ob/ob						
26458	SVVPHPGSRPDSLEDLL	Complement factor D	100	118	P03953	2045.07	35.9	0.031121543	0.78	1276.6	0.44	149.95	0.117460442	down-regulated in ob/ob						
26537	KNGTGpGpGpGpGpGAGEKGD	Collagen alpha-1(iii) chain	609	630	P08121	2049.01	36.99	0.007164724	0.89	366.3	0.22	19.23	0.052497952	down-regulated in ob/ob						
27104	AGRGAGEVpGpGpGAGEKGSgG	Collagen alpha-1(i) chain	905	927	P11087	2088.05	36.3	0.012142889	0.89	348	0.44	59.64	0.17137931	down-regulated in ob/ob						
27322	AGRpGpGpGpGpGAGEKGSgG	Collagen alpha-1(i) chain	905	927	P11087	2104.02	36.19	0.034018563	1	481.07	0.67	125.88	0.261666701	down-regulated in ob/ob						
27962	GpGpGpGpGpGAGEKpGpG	Collagen alpha-2(i) chain	499	520	Q01149	2149.08	28.16	0.020886117	1	331.28	0.22	66.41	0.200464864	down-regulated in ob/ob						
28672	TTGpGpGpGpGpGAGEKpGpG	Collagen alpha-2(i) chain	569	590	Q01149	2199.05	34.97	0.02550148	1	1454.78	1	975.7	0.670685602	down-regulated in ob/ob						
30714	SGTGTGpGpGAGEKpGpGAGEKpGpG	Collagen alpha-2(i) chain	567	590	Q01149	2343.17	37.04	0.039808966	0.89	2527.56	0.89	5404.25	2.138129263	up-regulated in ob/ob						
30739	PKSgDpGpGpGAGEKpGpGAGEKpGpG	Collagen alpha-2(i) chain	459	483	Q01149	2345.07	34.61	0.007501881	1	956.73	1	541.31	0.565791812	down-regulated in ob/ob						
32649	AVGGVQPPDAMVpGGLLEKpVFS	Napsin-A	190	213	O09043	2480.32	45.06	0.007501881	0.78	505.29	0	0	0	down-regulated in ob/ob						
34635	AVGGVQPPDAMVpGGLLEKpVFS	Napsin-A	190	214	O09043	2627.39	45.64	0.012142889	0.78	17651.2	0.11	9.66	0.000547272	down-regulated in ob/ob						
34793	AVGGVQPPDAMVpGGLLEKpVFS	Napsin-A	190	214	O09043	2643.38	45.91	0.004385248	0.89	4457.79	0	0	0	down-regulated in ob/ob						
35125	REGSpGAGEKpGpGAGEKpGAGEKpG	Collagen alpha-1(i) chain	1003	1030	P11087	2669.26	29.68	0.048049899	1	3031.72	0.89	5197.89	1.714501999	up-regulated in ob/ob						
36104	KNGETGpGpGpGAGEKpGpGAGEKpGpG	Collagen alpha-1(iii) chain	609	638	P08121	2742.29	39.65	0.031121543	1	3463.84	1	5616.43	1.621446141	up-regulated in ob/ob						
36597	GLpGpGpGAGEKpGAGEKpGAGEKpG	Collagen alpha-2(i) chain	562	590	Q01149	2780.39	38.92	0.048049899	0.89	664.51	0.89	1583.27	2.382612752	up-regulated in ob/ob						
41481	YLNRSSEGGDGLVGGSDpAHVpPPLTIP	Napsin-A	215	246	O09043	3371.6	41.55	0.007501881	0.78	2389.84	0	0	0	down-regulated in ob/ob						
43263	SAPpYKRWYDpVSPVPHGSRPDSLEDLL	Complement factor D	87	118	P03953	3664.78	33.12	0.007501881	0.78	8344.63	0	0	0	down-regulated in ob/ob						





13399	NGDDGEAGKpGrpG	Collagen alpha-1(I) chain	218	231	P11087	1357.65	31.57	0.01066665	1	1564.23	1	3037.37	1.941766876	up-regulated in db/db							
13864	WTDVGMSPRIES	Pro-epidermal growth factor	620	631	P01132	1376.73	37.67	0.002921538	1	96.82	0.09	10.07	0.104007436	down-regulated in db/db							
14373	AGPpGAPGAPpGPIG	Collagen alpha-1(I) chain	827	843	P11087	1397.73	48.13	0.01066665	1	809.54	1	1768.29	2.184314519	up-regulated in db/db							
14420	PGAKGepGDTGVKGD	Collagen alpha-1(I) chain	812	826	P11087	1399.71	33.42	0.00193307	1	3061.85	1	4985.28	1.628192106	up-regulated in db/db							
14770	QDQpGAKGepGDTGVKGD	Collagen alpha-1(I) chain	810	824	P11087	1412.74	31.8	0.046851511	1	2239.14	1	1880.29	0.839737578	down-regulated in db/db							
14858	GpGrpGpGpGpGpGpGpG	Collagen alpha-1(I) chain	174	188	P11087	1417.73	39.72	0.046004005	0.75	400.45	0.55	128.67	0.321313522	down-regulated in db/db							
14924	GpPpGpGpGpGpGpGpG	Collagen alpha-1(I) chain	321	336	P11087	1420.69	48.02	0.004667295	0.75	521.12	0	0	0	down-regulated in db/db							
15221	GEVpGpGpGpGpGpGpG	Collagen alpha-1(I) chain	909	924	P11087	1433.72	38.81	0.035804475	0.75	702.07	0.91	1537.19	2.189511017	up-regulated in db/db							
15293	GpPpGpGpGpGpGpGpG	Collagen alpha-1(I) chain	321	336	P11087	1436.7	48.08	0.001509036	1	3355.44	1	722	0.215172973	down-regulated in db/db							
15530	GRpGEVpGpGpGpGpGpG	Collagen alpha-1(I) chain	906	921	P11087	1445.74	39.5	0.006554586	0.5	672.46	1	2168.98	3.225440918	up-regulated in db/db							
16118	ESGSPEGNGSpGMPGP	Collagen alpha-1(I) chain	310	325	P28481	1471.67	48.22	0.030348005	0.75	245.51	0.18	31.66	0.128956051	down-regulated in db/db							
16128	VSiNKLQNSiD	Kidney androgen-regulated protein	25	37	P61110	1471.82	39.58	0.004309984	1	26067.23	0.55	675.95	0.025931025	down-regulated in db/db							
16332	GpPpGpGpGpGpGpGpG	Collagen alpha-1(I) chain	639	654	P11087	1480.71	39.19	0.004487973	1	1216.77	0.73	590.98	0.485695735	down-regulated in db/db							
16425	SiNKLQNSiDL	Kidney androgen-regulated protein	26	38	P61110	1485.84	39.49	0.002348934	1	5638.18	0.18	241.96	0.042914558	down-regulated in db/db							
16660	QVGEASLQFETLR	Serine protease inhibitor A3K	284	296	P07759	1497.91	37.83	0.030028334	1	74.58	0.27	21.15	0.283588093	down-regulated in db/db							
16733	GpPpGpGpGpGpGpGpG	Collagen alpha-2(I) chain	1096	1113	Q01149	1500.79	48.28	0.01066665	1	2831.95	1	1854.09	0.654704356	down-regulated in db/db							
16741	AHLNKGDTFQ	Major urinary protein 1	121	133	P11588	1500.77	32.08	0.006274818	1	383.34	1	897.59	2.341498409	up-regulated in db/db							
17232	KpGEQGVpDGLGApGp	Collagen alpha-1(I) chain	646	661	P11087	1522.78	40.4	0.031508511	1	2912.19	0.91	3798.09	1.304204053	up-regulated in db/db							
17342	DQGPpGAKGepDpGVK	Collagen alpha-1(I) chain	809	824	P11087	1527.78	33.82	0.046851511	1	702.02	1	1094.05	1.558431384	up-regulated in db/db							
17350	ALAHFDGILGLGFPT	Napsin-A	174	188	O09043	1527.82	38.48	0.046851511	1	1590.89	0.91	394.29	0.247842403	down-regulated in db/db							
17924	RDGApGAKGDRGETGP	Collagen alpha-1(I) chain	1015	1030	P11087	1555.8	28.13	0.021057571	1	1009.83	1	2316.36	2.29381181	up-regulated in db/db							
18066	SpSGSPDGKtGpGpGpG	Collagen alpha-1(I) chain	532	549	P11087	1563.79	40.57	0.002348934	0.13	4.18	1	1069.27	255.8062201	up-regulated in db/db							
18174	QDQpGAKGepGDTGVKGD	Collagen alpha-1(I) chain	810	826	P11087	1568.8	33.54	0.001509036	1	1062.57	1	2485.05	2.337165058	up-regulated in db/db							
18465	VSiNKLQNSiDL	Kidney androgen-regulated protein	25	38	P61110	1584.92	40.18	0.00193307	1	66953.46	1	6520.21	0.097384213	down-regulated in db/db							
18821	GpGpGpGpGpGpGpGpG	Collagen alpha-1(III) chain	497	513	P08121	1605.82	32.95	0.01066665	1	2130	1	9514.86	1.650169014	up-regulated in db/db							
18875	TGSpGpGpGpGpGpGpG	Collagen alpha-1(I) chain	530	547	P11087	1609.79	40.88	0.003271116	1	2758.37	1	4373.74	1.585624844	up-regulated in db/db							
19279	GpApGpSGFGLPpGpGpG	Collagen alpha-1(II) chain	657	674	P28481	1633.72	48.23	0.001509036	1	313.23	0	0	0	down-regulated in db/db							
19345	GSpSGpGpGpGpGpGpG	Collagen alpha-1(I) chain	531	549	P11087	1636.83	40.73	0.006274818	1	3894.08	1	5988.93	1.537957618	up-regulated in db/db							
19556	ATLNKTGAASVLGPK	Copper transport protein ATOX1	53	68	O08997	1646.9	28.02	0.001509036	1	154.05	0	0	0	down-regulated in db/db							
19559	QQAQpGpGpGpGpGpG	Collagen alpha-1(VII) chain	1267	1284	P63870	1646.84	40.3	0.004487973	1	8357.77	0.73	825.11	0.098723703	down-regulated in db/db							
19701	SGVGMGpGpGpGpGpGpG	Collagen alpha-1(III) chain	1663	181	P08121	1655.75	48.34	0.004973959	1	1191.2	0.45	188.59	0.158319342	down-regulated in db/db							
19814	GLpGpGpGpGpGpGpGpG	Collagen alpha-1(I) chain	633	650	P11087	1662.83	41	0.031508511	1	4052.25	1	5189.94	1.280755136	up-regulated in db/db							
19837	GpPpGpGpGpGpGpGpG	Collagen alpha-1(I) chain	321	339	P11087	1663.79	48.28	0.002862923	1	769.16	0.36	118.25	0.153651247	down-regulated in db/db							
19995	QpGVGpGpGpGpGpGpG	Collagen alpha-1(XVI) chain	436	452	Q08LX7	1671.65	48.03	0.004487973	0.75	1020.59	1	2987.63	2.898931086	up-regulated in db/db							
20402	DGKTGpGpGpGpGpGpG	Collagen alpha-1(I) chain	539	556	P11087	1691.85	35.18	0.001509036	1	340.67	1	1320.92	3.877418029	up-regulated in db/db							
20503	VSiNKLQNSiDL	Kidney androgen-regulated protein	25	39	P61110	1697.90	40.83	0.003593092	1	19694.1	0.82	2691.01	0.136640415	down-regulated in db/db							
20534	DQGPpGAKGepDpGVKGD	Collagen alpha-1(I) chain	809	826	P11087	1699.82	35.9	0.014560573	1	685.41	0.82	355.45	0.51895471	down-regulated in db/db							
20552	EDKDGSpEGpGpGpGpG	Collagen alpha-1(III) chain	462	479	P08121	1700.78	41.84	0.014560573	1	616.26	0.82	352.8	0.572485639	down-regulated in db/db							
20580	pGpGpGpGpGpGpGpGpG	Collagen alpha-2(I) chain	126	144	Q01149	1701.86	38.55	0.002348934	1	283	0.27	29.17	0.103074205	down-regulated in db/db							
20728	GmPpGpGpGpGpGpGpG	Collagen alpha-1(III) chain	536	554	P08121	1711.79	40.67	0.03002618	0.5	976.2	1	3138.62	3.21514034	up-regulated in db/db							
20796	DQGPpGAKGepDpGVKGD	Collagen alpha-1(I) chain	809	826	P11087	1715.82	35.95	0.014505996	1	921.43	0.73	436.77	0.474013219	down-regulated in db/db	0.030751954	0.73	436.77	0	0	0	down regulated in ACEI
21257	TGSpGpGpGpGpGpGpG	Collagen alpha-1(I) chain	530	549	P11087	1737.84	41.61	0.046851511	0.88	3616.54	0.91	5530.04	1.52909703	up-regulated in db/db							
21347	TGSpGpGpGpGpGpGpG	Uromodulin	509	505	Q11X17	1742.61	41.19	0.046851511	0.13	120.61	0.73	764.51	6.328694967	up-regulated in db/db							
21455	GTARGAPpGpGpGpGpG	Collagen alpha-1(I) chain	781	799	P11087	1747.81	36.04	0.031508511	0.88	76.87	0.18	27.91	0.363808526	down-regulated in db/db							
21480	KNGETGPpGpGpGpGpG	Collagen alpha-1(III) chain	609	627	P08121	1748.85	42.07	0.008235741	1	394.81	0.64	173.96	0.404061706	down-regulated in db/db							
21517	LSAPEYKRVRVDQ	Complement factor D	86	99	P03953	1750.85	33.74								0.03637941	0.91	893.67	0.56	268.98	0.300983585	down regulated in ACEI
21729	GpPpGpGpGpGpGpGpG	Collagen alpha-2(IV) chain	1210	1228	Q31962	1761.89	40.36	0.022100272	0.88	406.46	0.18	199.06	0.489740688	down-regulated in db/db							
21733	TGGEVpGpGpGpGpGpG	Collagen alpha-2(I) chain	569	585	Q01149	1761.9	33.73	0.006274818	1	1026.22	0.91	1836.43	1.789509072	up-regulated in db/db							
21810	EDHLWSDWAIPSVI	Pro-epidermal growth factor	700	714	P01132	1765.89	41.6	0.030348005	0.75	214.86	0.09	43.72	0.203481337	down-regulated in db/db							
21899	DQGPpGAKGepDpGVKGD	Collagen alpha-1(I) chain	809	827	P11087	1770.89	35.47	0.021057571	1	679.12	1	920.15	1.354915384	up-regulated in db/db							
22065	VLNKDSGDSGGELVLS	Napsin-A	215	231	O09043	1779.88	41.85	0.001509036	1	490.82	1	1687.45	3.438022085	up-regulated in db/db							
22220	DQGPpGAKGepDpGVKGD	Collagen alpha-1(I) chain	809	827	P11087	1786.86	35.6	0.00193307	1	932	1	1636.7	1.75611588	up-regulated in db/db							
22305	GAHGEDDWPVAVHL	Vacuolar protein sorting-associated protein 13C	2646	2661	Q08X70	1791.9	35	0.00842438	0.75	231.9	0.09	10.08	0.043467012	down-regulated in db/db							
22694	SpGRDpGpGpGpGpGpG	Collagen alpha-1(I) chain	1012	1030	P11087	1812.91	29.3	0.043022835	1	203.26	0.82	419.34	2.063071928	up-regulated in db/db							
22729	pGpApGpGpGpGpGpGpG	Collagen alpha-1(XXII) chain	357	375	Q8K462	1814.9	41.54	0.021057571	1	1394.75	1	937.78	0.672364223	down-regulated in db/db							
22880	VGEKpGpGpGpGpGpGpG	Collagen alpha-2(I) chain	849	869	Q01149	1824.89	42.14	0.004786026	0.88	563.1	1	1687.86	2.997442728	up-regulated in db/db							
23042	GpPpGpGpGpGpGpGpG	Collagen alpha-1(III) chain	641	660	P08121	1834.89	41.58	0.001509036	1	2510.82	1	5195.54	2.069260242	up-regulated in db/db							
23356	HELKASDpYDRNVEL	ATP-binding cassette sub-family A member 13	1292	1307	Q55569	1849.93	34.64	0.002358894	0.75	442.18	1	3655.45	8.26688265	up-regulated in db/db							
23484	ADGpGpGpGpGpGpGpG	Collagen alpha-1(I) chain	808	827	P11087	1857.92	35.06	0.038867999	1	291.29	0.91	671.06	2.303752274	up-regulated in db/db							
23764	SLLKHPNIAVDPIERL	Pro-epidermal growth factor	162	178	P01132	1875.07	29.58	0.001509036	1	346.52	0	0	0	down-regulated in db/db							
23770	GpGpGpGpGpGpGpGpG	Collagen alpha-1(III) chain	764	784	P08121	1875.92	42.43	0.014505996	1	1102.74	0.73	600.28	0.544353157	down-regulated in db/db							
24239	ETGAPGpGpGpGpGpGpG	Collagen alpha-1(I) chain	901	921	P11087	1900.94	42.53	0.01324474	0.88	876.13	1	2061.45	2.352904249	up-regulated in db/db							
24713	ALHDpVESKIFFACTA	Pro-epidermal growth factor	522	538	P01132	1929.97	42.48	0.002348934	0.88	910.69	0	0	0	down-regulated in db/db							

1502027	SNIAVDPIERL	Pro-epidermal growth factor	168	178	P01132	1225,72	39,95	0,002348934	1	3806,75	0,18	88,1	0,023143101	down-regulated in db/db							
1502180	LKWIERANMD	Pro-epidermal growth factor	539	548	P01132	1274,63	29,99	0,00193307	1	954,92	1	2645,97	2,77088133	up-regulated in db/db							
1504057	KNRDDGEAGKpGRpGERGPPGp	Collagen alpha-1(I) chain	217	238	P11087	2192,09	27,74	0,001509036	1	577,86	1	1322,75	2,289049251	up-regulated in db/db	0,030751954	1	1322,75	0,89	788,79	0,596325836	down regulated in ACEI

reversed by ACEI treatment

Supplementary Table 3: Sequences of the 51 identical peptides in the two T2D nephropathy mouse strains.

Peptide_ID	Sequence	Protein name	Adjusted pValue BTBRob/ob/B TBR	FOLD CHANGE BTBRob/ob/B TBR	DIRECTION BTBRob/ob/B TBR	Adjusted pValue db/db / db/m	FOLD CHANGE db/db / db/m	DIRECTION db/db / db/m
1127	ApGERGPPG	Collagen alpha-1(III) chain	0,004385248	0,067946968	down-regulated in ob/ob	0,01324474	0,347291827	down-regulated in db/db
3062	GQpGEKGPpG	Collagen alpha-1(III) chain	0,007164724	0,068955079	down-regulated in ob/ob	0,00803187	0,126335911	down-regulated in db/db
3144	GPPGESGREG	Collagen alpha-1(I) chain	0,003740306	0	down-regulated in ob/ob	0,04685151	0,431706687	down-regulated in db/db
4520	ASLQPETLR	Serine protease inhibitor A3K	0,004385248	0	down-regulated in ob/ob	0,0046673	0	down-regulated in db/db
4882	GQPgAKGEpGD	Collagen alpha-1(I) chain	0,017010274	19,1167019	up-regulated in ob/ob	0,00627482	2,137709905	up-regulated in db/db
5204	SpGPDGKTGPP	Collagen alpha-1(I) chain	0,009919353	0,286652113	down-regulated in ob/ob	0,00478603	0,488928177	down-regulated in db/db
5677	ApGDRGEAGPP	Collagen alpha-1(I) chain	0,002949087	0,355568396	down-regulated in ob/ob	0,01032199	0,447450809	down-regulated in db/db
5886	GPPGPTGPTGPP	Collagen alpha-1(I) chain	0,005037542	0,068343455	down-regulated in ob/ob	0,01095537	0,24759554	down-regulated in db/db
7020	DQTRVLNLGP	Uromodulin	0,00768409	6,595290932	up-regulated in ob/ob	0,01212327	3,772924501	up-regulated in db/db
7064	GpPGSpGSpGEQ	Collagen alpha-1(I) chain	0,004344693	0,015971149	down-regulated in ob/ob	0,03580448	0,554707921	down-regulated in db/db
7194	GPPGPTGPTGPPG	Collagen alpha-1(I) chain	0,014205913	0,116544308	down-regulated in ob/ob	0,00234893	0,12	down-regulated in db/db
7213	GpGERGEHGPP	Collagen alpha-1(III) chain	0,023549868	0,347919643	down-regulated in ob/ob	0,00627482	0,632485158	down-regulated in db/db
7366	FLEQIHVLE	Major urinary protein 1	0,004385248	0,045690793	down-regulated in ob/ob	0,00842438	0,010799481	down-regulated in db/db
7814	DGApGAKGDRGE	Collagen alpha-1(I) chain	0,031121543	0,653932776	down-regulated in ob/ob	0,00446696	0,651631784	down-regulated in db/db
8738	ApGEKGEggPPGP	Collagen alpha-1(III) chain	0,012479191	0,493380476	down-regulated in ob/ob	0,00150904	0,526555583	down-regulated in db/db
9139	SpQRGEpPQPG	Collagen alpha-1(III) chain	0,014018563	0,550282216	down-regulated in ob/ob	0,00150904	0,54523033	down-regulated in db/db
9523	GPPGESGREGSpG	Collagen alpha-1(I) chain	0,004385248	0,6529115	down-regulated in ob/ob	0,038868	1,882634368	up-regulated in db/db
10290	VSINKELQNSI	Kidney androgen-regulated protein	0,005541668	0,075043906	down-regulated in ob/ob	0,00842438	0,205824815	down-regulated in db/db
10734	RpGEVGPpGPPGP	Collagen alpha-1(I) chain	0,003485285	1,767827506	up-regulated in ob/ob	0,00446696	1,666494353	up-regulated in db/db
10940	DGKTGPpGpAGQDG	Collagen alpha-1(I) chain	0,013313568	0,227362675	down-regulated in ob/ob	0,00226331	0,081662033	down-regulated in db/db
11018	GpPGPPpGPPSSGG	Collagen alpha-1(I) chain	0,003740306	0	down-regulated in ob/ob	0,00446696	0,044921875	down-regulated in db/db
12726	GGpGERGEHGPPGP	Collagen alpha-1(III) chain	0,014018563	3,416227899	up-regulated in ob/ob	0,04685151	1,498340417	up-regulated in db/db
12934	KLGVGSLQELAPQ	Sperm flagellar protein 1	0,007501881	0	down-regulated in ob/ob	0,00265809	0,026862169	down-regulated in db/db
13399	NGDDGEAGKpGRpG	Collagen alpha-1(I) chain	0,012479191	0,568244322	down-regulated in ob/ob	0,01066665	1,941766876	up-regulated in db/db
13864	WTDVGMSPRIES	Pro-epidermal growth factor	0,012142689	0,0572305	down-regulated in ob/ob	0,00292154	0,104007436	down-regulated in db/db
14770	GQPGAKGEpGDTGVK	Collagen alpha-1(I) chain	0,005095706	0,576090512	down-regulated in ob/ob	0,04685151	0,839737578	down-regulated in db/db
15293	GpPGPTGPTGPPGFPpG	Collagen alpha-1(I) chain	0,004385248	0,111575856	down-regulated in ob/ob	0,00150904	0,215172973	down-regulated in db/db
16425	SINKELQNSIDL	Kidney androgen-regulated protein	0,004344693	0,00043387	down-regulated in ob/ob	0,00234893	0,042914558	down-regulated in db/db
16733	GPPpGPPpGPPGVSGGG	Collagen alpha-2(I) chain	0,012142689	0,186853199	down-regulated in ob/ob	0,01066665	0,654704356	down-regulated in db/db
16741	AHLINKEKDGETFQ	Major urinary protein 1	0,019906338	1,865123623	up-regulated in ob/ob	0,00627482	2,341498409	up-regulated in db/db
17232	KpGEQGVpGDLGApGP	Collagen alpha-1(I) chain	0,007501881	1,77331812	up-regulated in ob/ob	0,03150851	1,304204053	up-regulated in db/db
17342	DGQPGAKGEpGDTGVK	Collagen alpha-1(I) chain	0,010033808	0,581216252	down-regulated in ob/ob	0,04685151	1,558431384	up-regulated in db/db
18066	SpGSPGDGKTGPPGpAG	Collagen alpha-1(I) chain	0,012479191	2,436260312	up-regulated in ob/ob	0,00234893	255,8062201	up-regulated in db/db
18466	VSINKELQNSIDL	Kidney androgen-regulated protein	0,005603303	0,011215296	down-regulated in ob/ob	0,00193307	0,097384213	down-regulated in db/db

19345	GSpGSpGPDGKTGPpGPAG	Collagen alpha-1(I) chain	0,012479191	1,595414073	up-regulated in ob/ob	0,00627482	1,537957618	up-regulated in db/db
19814	GLpGPAGPpGEAGKpGGEQ	Collagen alpha-1(I) chain	0,002949087	1,894155813	up-regulated in ob/ob	0,03150851	1,280755136	up-regulated in db/db
20503	VSINKELQNSIIDLL	Kidney androgen-regulated protein	0,003740306	0	down-regulated in ob/ob	0,00359309	0,136640415	down-regulated in db/db
21455	pTGARGAPDRGEAGPPGp	Collagen alpha-1(I) chain	0,04691826	0,278216144	down-regulated in ob/ob	0,03150851	0,363080526	down-regulated in db/db
21893	DGQPGAKGEpGDTGVKGDA	Collagen alpha-1(I) chain	0,003485285	2,299822236	up-regulated in ob/ob	0,02105757	1,354915184	up-regulated in db/db
22065	YLNRDSEGSDDGELVLG	Napsin-A	0,003740306	1,892375657	up-regulated in ob/ob	0,00150904	3,438022085	up-regulated in db/db
22220	DGQpGAKGEpGDTGVKGDA	Collagen alpha-1(I) chain	0,004385248	1,658928402	up-regulated in ob/ob	0,00193307	1,75611588	up-regulated in db/db
22880	VGEKGPSGEpGTAGApGTAGP	Collagen alpha-2(I) chain	0,02550148	2,14178134	up-regulated in ob/ob	0,00478603	2,997442728	up-regulated in db/db
23042	GlpGTGGPpGENGKpGEPGP	Collagen alpha-1(III) chain	0,012479191	1,794985985	up-regulated in ob/ob	0,00150904	2,069260242	up-regulated in db/db
23356	IELSKASYVDRNVEL	ATP-binding cassette sub-family A member	0,012479191	5,4412103	up-regulated in ob/ob	0,00235889	8,266882265	up-regulated in db/db
23770	GPIGPpGPAGQpGDKGEGGSp	Collagen alpha-1(III) chain	0,007164724	0,256758155	down-regulated in ob/ob	0,014506	0,544353157	down-regulated in db/db
24239	ETGPAGRpGEVGPpGPpGPAG	Collagen alpha-1(I) chain	0,003740306	2,447651697	up-regulated in ob/ob	0,01324474	2,352904249	up-regulated in db/db
24713	ALDYDPVESKIYFAQTA	Pro-epidermal growth factor	0,005603303	0,00297948	down-regulated in ob/ob	0,00234893	0	down-regulated in db/db
25110	VVPHPGSRPDSLEDDLIL	Complement factor D	0,004385248	0,001240732	down-regulated in ob/ob	0,039009	0,169630911	down-regulated in db/db
26537	KNGETGPQGPpGPTGPAGDKGD	Collagen alpha-1(III) chain	0,007164724	0,052497952	down-regulated in ob/ob	0,00226331	0,103278558	down-regulated in db/db
30714	SGTTGEVGKpGERGLpGEFGLpGP	Collagen alpha-2(I) chain	0,039808966	2,138129263	up-regulated in ob/ob	0,02595266	1,43246881	up-regulated in db/db
35125	REGSpGAEGSpGRDGApGAKGDRGETGP	Collagen alpha-1(I) chain	0,048043989	1,714501999	up-regulated in ob/ob	0,00921957	4,098392283	up-regulated in db/db

Supplementary Table 4: Overlap between peptides responding to RASi in two different T2D mouse strains. RASi treatment modified the abundance of 4 identical peptides (out of 11 and 18 peptides for the BTBRob/ob and UNxdb/db strains, respectively) that were all changed in the same direction in the two T2D strains. RASi, enalapril.

PeptideID	Sequence	Protein name	Start	Stop	Uniprot	Adjusted pValue	Fold change BTBRob/ob+RASi	Adjusted pValue	Fold change UNxdb/db+RASi	Regulation by RASi
2465	QVSPGAKmP	Transcription factor SOX-6	378	386	P40645	0,025	130,23	0,007	23,75	Up
5677	ApGDRGEAGPp	Collagen alpha-1(I) chain	787	797	P11087	0,038	0,05	0,018	Absent in UNxdb/db+RASi	Down
10361	KGEpGDTGVKGD	Collagen alpha-1(I) chain	815	827	P11087	0,019	Absent in BTBRob/ob+RASi	0,007	Absent in UNxdb/db+RASi	Down
12099	LGPYVAVFDRGD	Napsin-A	373	384	O09043	0,022	1521,42	0,007	1405,12	Up



Supplementary Table 6: The 21 differentially excreted peptides identified and used for the generation of the humanized classifier and their respective human ortholog identified in CKD273. Bold: orthology. RASi, enalapril.

Peptide ID	Sequence	Protein name	Regulation Diab/Non diab	Regulation Diab+RASi/Diab	Ortholog CKD273		
					Regulation in patients	CKD273 ID	Human sequence
710	SpGRDGApG	Collagen alpha-1(I) chain	Down		Down	39163	<b>SpGRDGSpGAKGDRG</b>
1127	ApGERGPPG	Collagen alpha-1(III) chain	Down		Down	84440	<b>KGDAGApGApGGKGDAGApGERGPPG</b>
3062	GQpGEKGPpG	Collagen alpha-1(III) chain	Down		Down	133849	<b>NTGApGSpGVSGPKGDAGQPPGkGSPAQQPpGApGpLG</b>
3438	DGKTGPpGPAG	Collagen alpha-1(I) chain	Down		Down	5675	<b>DGKTGPpGPA</b>
4497	SpQRGEpGP	Collagen alpha-1(III) chain		Up	Down	55523	<b>SpGSNGApGQRGEpGPQG</b>
5599	ApGKDGPPGPAG	Collagen alpha-1(III) chain		Down	Down	76415	<b>SNGNpGpPGPSGSPGKDGPPGpAG</b>
5677	ApGDRGEAGPp	Collagen alpha-1(I) chain	Down		Down	17694	<b>ApGDRGEpGpP</b>
8738	ApGEKGEPPpGP	Collagen alpha-1(III) chain	Down		Down	77184	<b>NGEpGGKGERGApGEKGEPPpG</b>
9139	SpQRGEpGPQG	Collagen alpha-1(III) chain	Down		Down	55523	<b>SpGSNGApGQRGEpGPQG</b>
10361	KGEpGDTGVKGDA	Collagen alpha-1(I) chain		Down	Up	97506	<b>GPpGADGQpPGAKGEpGDAGAKGDAGpPGP</b>
10514	ApGEKGEPPpGPA	Collagen alpha-1(III) chain	Down		Down	87460	<b>GQNGEpGGKGERGApGEKGEPPpG</b>
11018	GpPGPpGPpGPPSSG	Collagen alpha-1(I) chain	Down		Down	20756	<b>GpGpPGPPGPPS</b>
12554	GPpGPTGPAGDKGDS	Collagen alpha-1(III) chain		Down	Up	32343	<b>TGPGGDKGDTGPpGP</b>
16857	KpGEQGVPGDLGApGP	Collagen alpha-1(I) chain	Up		Up	58941	<b>GPpGEAGKpGEQGVpDGLG</b>
19345	GSpSspGPDGKTGPpGPAG	Collagen alpha-1(I) chain	Up		Up	48106	<b>SpGSspGPDGKTGPpGpAG</b>
19814	GLpGPAGPpGEAGKpGEQ	Collagen alpha-1(I) chain	Up		Up	58941	<b>GPpGEAGKpGEQGVpDGLG</b>
21893	DGQPGAKGEpGDTGVKGDA	Collagen alpha-1(I) chain	Up		Up	80891	<b>ADGQPGAKGEpGDAGAKGDAGPPGp</b>
22220	DGQpGAKGEpGDTGVKGDA	Collagen alpha-1(I) chain	Up		Up	77018	<b>DGQPGAKGEpGDAGAKGDAGPPGp</b>
23042	GlpGTGGPpGENGKpGEpGP	Collagen alpha-1(III) chain	Up		Up	61304	<b>GlpGTGGPpGENGKpGEpGP</b>
26537	KNGETGPQGPpGPTGPAGDKGD	Collagen alpha-1(III) chain	Down		Down	107460	<b>KNGETGPQGPpGPTGPAGDKGDGPpGpQG</b>
27104	AGRpGEVGPpGPpGPAKEKSpG	Collagen alpha-1(I) chain	Down		Down	108724	<b>KEGGKGRGETGPAGRpGEVGPpGPpGPAG</b>